World Journal of Radiology

Submit a Manuscript: http://www.wjgnet.com/esps/
Help Desk: http://www.wjgnet.com/esps/helpdesk.aspx
DOI: 10.4329/wjr.v7.i6.110

World J Radiol 2015 June 28; 7(6): 110-127
ISSN 1949-8470 (online)

EDITORIAL

Advances of multidetector computed tomography in the characterization and staging of renal cell carcinoma

Athina C Tsili, Maria I Argyropoulou

Athina C Tsili, Maria I Argyropoulou, Department of Radiology, Medical School, University of Ioannina, 45110 Ioannina, Greece

Author contributions: Tsili AC and Argyropoulou MI contributed to this paper.

Conflict-of-interest: None.

Correspondence to: Athina C Tsili, MD, Assistant Professor, Department of Radiology, Medical School, University of Ioannina, Leoforos Panepistimiou, 45110 Ioannina, Greece. a_tsili@yahoo.gr
Telephone: +30-697-6510904
Fax: +30-265-1007862

Received: January 30, 2015
Peer-review started: January 31, 2015
First decision: February 7, 2015
Revised: March 18, 2015
Accepted: April 27, 2015
Article in press: April 29, 2015
Published online: June 28, 2015

Abstract

Renal cell carcinoma (RCC) accounts for approximately 90%-95% of kidney tumors. With the widespread use of cross-sectional imaging modalities, more than half of RCCs are detected incidentally, often diagnosed at an early stage. This may allow the planning of more conservative treatment strategies. Computed tomography (CT) is considered the examination of choice for the detection and staging of RCC. Multidetector CT (MDCT) with the improvement of spatial resolution and the ability to obtain multiphase imaging, multiplanar and three-dimensional reconstructions in any desired plane brought about further improvement in the evaluation of RCC. Differentiation of RCC from benign renal tumors based on MDCT features is improved. Tumor enhancement characteristics on MDCT have been found closely to correlate with the histologic subtype of RCC, the nuclear grade and the cytogenetic characteristics of clear cell RCC. Important information, including tumor size, localization, and organ involvement, presence and extent of venous thrombus, possible invasion of adjacent organs or lymph nodes, and presence of distant metastases are provided by MDCT examination. The preoperative evaluation of patients with RCC was improved by depicting the presence or absence of renal pseudocapsule and by assessing the possible neoplastic infiltration of the perirenal fat tissue and/or renal sinus fat compartment.

Key words: Carcinoma; Kidney; Computed tomography; Renal cell carcinoma; Staging; Multidetector computed tomography

Core tip: Multidetector computed tomography (MDCT) remains the most widely available and most effective modality for the detection and staging of renal cell carcinoma (RCC), with a staging accuracy up to 91%. MDCT scanners with the improvement of spatial resolution and the ability to obtain multiplanar and 3D-reconstructions greatly improved the diagnostic performance of CT in characterizing RCC and estimating the extent of the disease. Important information for treatment planning is provided by CT examination, including tumor location and size, renal arterial and venous anatomy and relationship to the pelvicaliceal system.

Tsili AC, Argyropoulou MI. Advances of multidetector computed tomography in the characterization and staging of renal cell carcinoma. *World J Radiol* 2015; 7(6): 110-127 Available from: URL: http://www.wjgnet.com/1949-8470/full/v7/i6/110.htm DOI: http://dx.doi.org/10.4329/wjr.v7.i6.110

INTRODUCTION

Renal cell carcinoma (RCC) represents the commonest primary malignancy of the kidney, accounting for about 2%-3% of all cancers[1-3]. In 2012, approximately 84400 new cases of RCC were diagnosed within the European Union and 34700 kidney cancer-related deaths occurred[2]. The estimated number of new cases of kidney cancer in the United States during 2014 was 63920, the great majority representing RCCs, accounting for the seventh most common malignancy in men and the 12th commonest malignancy in women[3]. An estimated 13860 deaths from kidney cancer were expected to occur in 2014[3].

The widespread use of cross-sectional imaging modalities has resulted in incidental detection of more than 50% of RCCs[1-4]. These tumors are often small, of low stage and grade, and therefore have a better prognosis[1-4]. Early-stage RCC is usually asymptomatic. The classic clinical triad of flank pain, gross haematuria, and palpable abdominal mass is not common (6%-10% of cases) and usually correlates with aggressive histology and advanced-stage disease[1,5,6]. There is a 1.5:1 predominance in men over women, with a peak incidence occurring during the 6th and 7th decades of life. The main predisposing factors for renal cancer are smoking, obesity, hypertension, chronic renal failure, chemical exposure and radiation exposure[1-3]. Heredity also plays a role, with approximately 4% of all RCCs seen in patients with an underlying tumor syndrome[7,8].

In patients with RCC, tumor stage at diagnosis, nuclear grade according to Fuhrman, and histologic subtype represent the most important prognostic factors[1]. Tumor stage greatly affects patient's prognosis and survival, and has an important impact on treatment planning. The tumor, node, metastasis (TNM) staging classification system is most commonly used, closely correlating with potential curability of the disease and prognosis[1,9]. The latest version of the TNM classification was published in 2010[1,9] and is presented in Table 1.

The grading classification of RCC is based on the microscopic characteristics of the neoplasm with hematoxylin and eosin staining. Fuhrman nuclear grade is the most widely accepted histological grading system for RCC[10]. Although affected by intra- and inter-observer discrepancies, it represents one of the most significant prognostic variables in patients with all stages of RCC[10-13]. This system categorizes RCC with grades 1, 2, 3, and 4, varying from tumors with small, round hyperchromatic nuclei, no visible nucleoli and little detail in the chromatin to those with larger, pleomorphic nuclei, single or multiple macronucleoli and coarsely granular chromatin[10]. Some researchers have simplified the Fuhrman grading system in order to improve interobserver reproducibility. More specifically, a modified two- or three-tiered Fuhrman grading system could probably have a virtually equal accuracy as the conventional 4-tiered Fuhrman grading system in predicting cancer-specific mortality[11-13].

The 2004 World Health Organization classification for renal neoplasms recognizes several distinct histologic subtypes of RCC, of which three main types are important: conventional (clear cell) RCC (ccRCC, accounting for approximately 80%-90% of RCCs); papillary RCC (10%-15%); and chromophobe RCC (4%-5%)[14,15]. In univariate analysis, there is a trend towards a better prognosis for patients with chromophobe *vs* papillary *vs* conventional RCC[16,17].

The 5-year overall survival for all types of RCC is 49%. More than half of cases are diagnosed at early-stage, for which the 5-year relative survival rate is 92%[1].

Radical nephrectomy with ipsilateral adrenalectomy, as established by Robson, was the treatment of choice since 1969[1]. During the last decades, there is a growing trend for more limited surgical resection, such as adrenal-sparing radical nephrectomy, laparoscopic nephrectomy, or nephron-sparing partial nephrectomy[1-4,18-24]. Partial nephrectomy can be performed, either with an open, pure laparoscopic or robot-assisted approach, based on surgeon's expertise and skills. Similar oncological outcomes have been reported for both nephron-sparing surgery (NSS) and radical nephrectomy[1,22-24]. NSS is primarily recommended in patients with T1a tumors, and when technically feasible in T1b neoplasms[1]. Non-surgical treatment, including ablative techniques such as cryoablation, and radiofrequency ablation have been proposed for RCCs less than 4 cm in diameter[1,25]. However, due to the low quality of the available data no published recommendations still exist on these techniques[1]. Active surveillance may be offered to some patients, especially in elderly and/or comorbid patients with small renal tumors[26,27].

ROLE OF COMPUTED TOMOGRAPHY

Computed tomography (CT) is widely accepted as the examination of choice for the detection, characterization and staging of RCC, with a staging accuracy up to 91%[4,28-47]. The wide availability of CT and its relative ease of performance and interpretation compared with magnetic resonance imaging (MRI) render it the main imaging method for staging RCC. In surgical cases, accurate preoperative imaging and exact tumor staging is of paramount importance for planning the optimal surgical approach and strategy, and for providing accurate prognostic information for the patient. Knowledge of the renal and tumor vascular supply and the relationship of the neoplasm to the adjacent renal

Table 1 New tumor, node, metastasis classification system for renal cell carcinoma

T-primary tumor			
Tx	Primary tumour cannot be assessed		
T0	No evidence of primary tumour		
T1	Tumour ≤ 7 cm in greatest dimension, limited to kidney		
T1a	Tumour ≤ 4 cm in greatest dimension, limited to kidney		
T1b	Tumour > 4 cm but ≤ 7 cm in greatest dimension, limited to kidney		
T2	Tumour > 7 cm in greatest dimension, limited to kidney		
T2a	Tumour > 7 cm but ≤ 10 cm in greatest dimension, limited to kidney		
T2b	Tumour > 10 cm in greatest dimension, limited to kidney		
T3	Tumour extends into major veins or perinephric tissues but not into the ipsilateral adrenal gland and not beyond Gerota fascia		
T3a	Tumour grossly extends into the renal vein or its segmental branches, or tumour invades perirenal and/or renal sinus fat but not beyond Gerota fascia		
T3b	Tumour grossly extends into the vena cava below the diaphragm		
T3c	Tumour grossly extends into the vena cava above the diaphragm or invades the wall of the vena cava		
T4	Tumour invades beyond Gerota's fascia (including contiguous extension into the ipsilateral adrenal gland)		
N-regional lymph nodes			
Nx	Regional nodes cannot be assessed		
N0	No regional lymph nodes metastases		
N1	Metastases in a single regional lymph node		
N2	Metastases in more than 1 regional lymph node		
M-distant metastases			
M0	No distant metastases		
M1	Distant metastases		
TNM stage grouping			
Stage Ⅰ	T1	N0	M0
Stage Ⅱ	T2	N0	M0
Stage Ⅲ	T3	N0	M0
	T1,T2,T3	N1	M0
Stage Ⅳ	T4	Any N	M0
	Any T	N2	M0
	Any T	Any N	M1

TNM: Tumor, node, metastasis.

parenchyma and the pelvicaliceal system are crucial for operative planning, particularly in patients planned for NSS[48-51].

According to the recommendations by the American College of Radiology, multidetector, multiphasic CT of the abdomen is considered appropriate for staging of small or incidentally detected renal tumors (equal or smaller than 3 cm in diameter)[52]. For renal tumors larger than 3 cm in diameter, multidetector CT (MDCT) is the diagnostic modality of choice. MRI of the abdomen is a suitable substitute, when patient cannot undergo contrast-enhanced CT. Ultrasonography may be considered more appropriate for staging small renal tumors, when the intravenous administration of contrast medium is contraindicated. Positron emission tomography (PET) does not yet have an established role in staging RCC. PET with the tracer fluorine-18-2-fluoro-2-deoxy-D-glucose-PET may find difficulties even in the detection of primary carcinoma against the normal background of hyperactivity in the kidneys. PET may be used as a complementary examination for confirming metastatic disease in lesions detected by CT, MRI, or bone scan, and it may be used to detect unsuspected metastases in high-risk patients[52].

The most recent technical advances introduced with the use of MDCT scanners brought about further advancements in the preoperative evaluation of RCC[4,31-51]. The main advantages of MDCT are fast scanning time, increased volume coverage, acquisition of thin slices and improved spatial and temporal resolution. Rapid coverage of the kidneys and scanning during specific organ perfusion phases after the intravenous administration of iodinated contrast material has improved the diagnostic performance of CT in the detection and characterization of renal masses[34-41]. The use of thin slices and the acquisition of near-isotropic or isotropic data improve the quality of volume data set for workstation analysis and multiplanar reformations (MPRs) and 3D reconstructions in any desired plane with excellent anatomic details are possible[30-33,49-51].

MDCT protocol

MDCT examination in cases of a known or suspected renal mass should include multiple phases, proper timing of each post-contrast enhanced phase, and use of MPRs and 3D-reconstructions. The CT protocol includes an unenhanced acquisition, combined with two or more post-contrast enhanced series (corticomedullary phase, nephrographic phase, and excretory phase)[4,28-47].

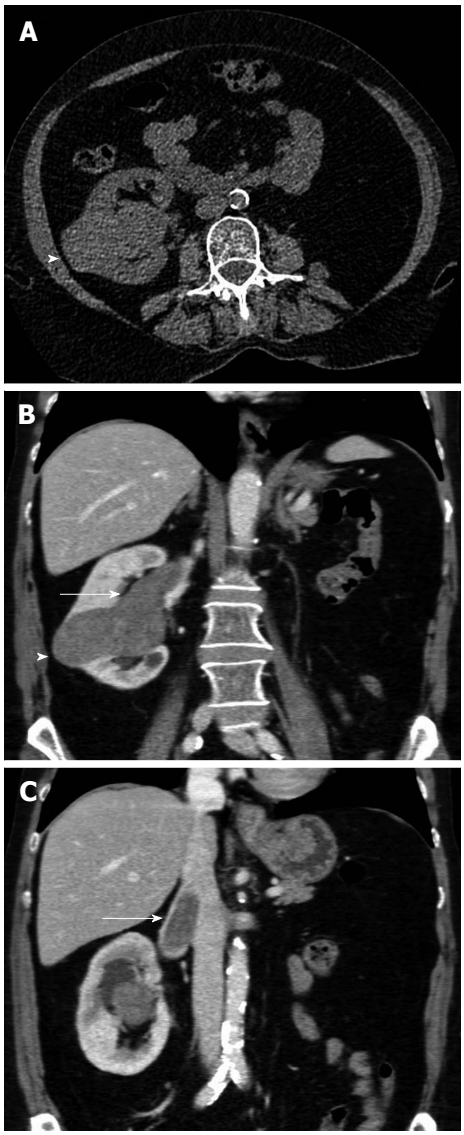

Figure 1 The 65-year-old woman with papillary renal cell carcinoma of the right kidney and tumoral invasion of the ipsilateral renal vein and the inferior vena cava (stage T3b, grade 2). The patient had left radical nephrectomy years ago for renal cell carcinoma. A: Transverse unenhanced computed tomography (CT) image shows a lobular right renal mass (arrowhead), located in the interlobar region. The mass is relatively homogeneous, slightly hyperdense (CT density: 40 HU), when compared to the normal renal parenchyma; B and C: Contrast-enhanced coronal multiplanar reformations during the corticomedullary phase depict right renal tumor, with moderate, homogeneous enhancement (arrowhead, mean CT density: 65 HU). Venous tumour thrombus is diagnosed as a filling defect within right renal vein and the infrahepatic part of the inferior vena cana (arrow). Neoplastic thrombus is seen extending directly from the neoplasm, enhancing with a similar pattern with primary malignancy.

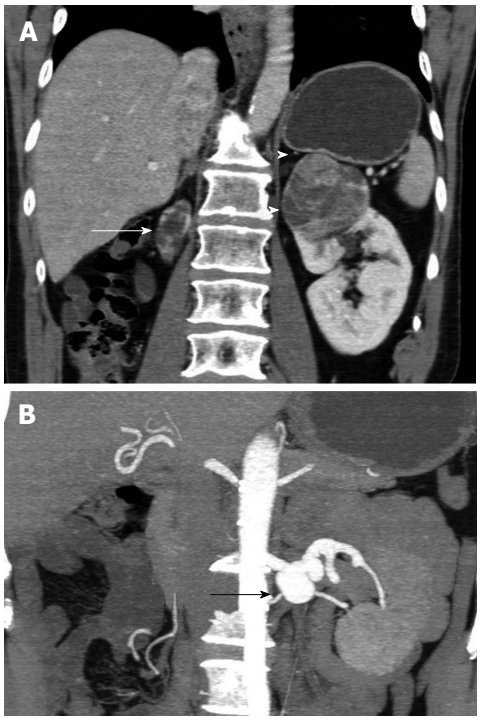

Figure 2 The 70-year-old man with clear cell renal cell carcinoma of the left solitary functioning kidney (stage T1b, grade 2). A: Post-contrast enhanced coronal multiplanar reformation during the corticomedullary phase depicts left upper pole renal mass, strongly and heterogeneously enhancing, after contrast material administration. A thin hyperdense rim (arrowheads) is detected around the tumor, proved to correspond to fibrous pseudocapsule on pathology. Atrophic right kidney (arrow); B: Coronal 3D-reconstruction during the same phase, using maximum intensity projection algorithm shows left renal artery aneurysm (arrow).

The unenhanced scanning is always necessary to serve as a baseline for measurements of enhancement after contrast material administration. Areas of hemorrhage and/or presence of calcifications are also seen on these images. In the corticomedullary phase, obtained 25-70 s after the start of injection, an intense enhancement of the renal cortex is observed, while the medulla does not enhance and remains hypodense. This phase is essential for staging RCC. An accurate diagnosis of venous extension of tumoral tissue is possible (Figure 1). This phase may be also used as a map for the delineation of the arterial anatomy of the kidneys (Figure 2), especially helpful in selected cases to plan NSS. Hypervascular arterialized metastases from RCC may be more evident on this phase (Figure 3). The nephrographic phase, with a delay of 80-180 s after contrast administration is considered the most important for detecting and characterizing renal tumors. During this phase, normal renal parenchyma enhances homogeneously, allowing the best opportunity for the delineation of renal masses, which are often detected with relatively less contrast enhancement (Figure 4). The excretory phase is acquired after a 4-8 min delay, resulting in excretion of contrast material into the pelvicaliceal system. The relationship of the tumor to the renal collecting system (Figure 5) and possible signs of invasion are evaluated in this acquisition.

In addition to multiphase imaging, multiplanar display techniques, including MPRs and 3D-reconstructions, more often with maximum intensity projection and volume rendering technique are essential and improve the diagnostic performance of CT in detecting, characterizing and staging of RCC[28-33,48-51]. MPRs and 3D-reconstructions can be viewed in multiple planes and orientations, providing a useful interctive road map when planning treatment, either surgery or conservative. Accurate depiction of the position of the kidney relative to the

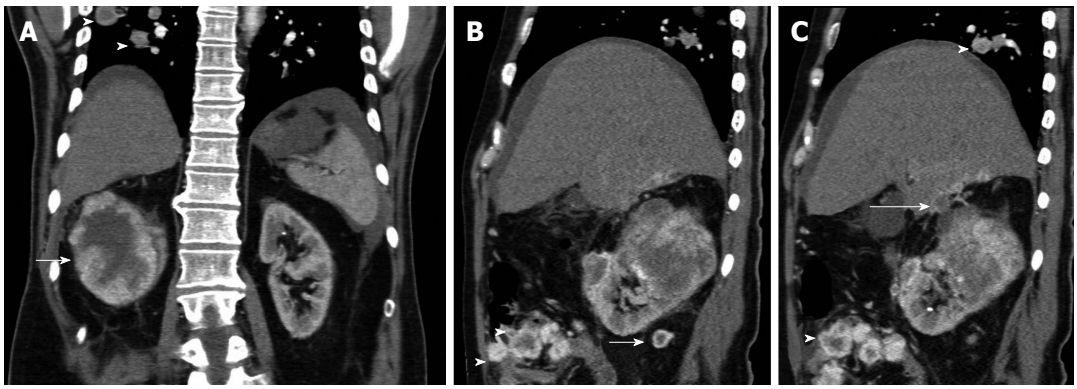

Figure 3 The 52-year-old man with advanced-stage clear cell renal cell carcinoma of the right kidney. Contrast-enhanced (A) coronal and (B and C) sagittal reformations during the corticomedullar phase show a large right renal tumor (arrow), strongly and inhomogeneously enhancing. Central hypodense parts within malignancy corresponded to areas of necrosis on histology. There is perinephric stranding and contrast-enhancing nodules in the perinephric fat (long arrow, B), a finding strongly suggestive for PR fat invasion. The tumor is seen extending and invading the undersurface of the liver (long arrow, C). Lung metastases are detected (arrowheads, A and C). There is also a small amount of ascites and nodular peritoneal masses (arrowheads, B), with heterogeneous enhancement, identical to that of the primary neoplasm, findings suggestive of peritoneal metastases. Peritoneal metastases from renal cell carcinoma (RCC) are extremely rare. Neoplastic invasion of the peritoneum by RCC may occur either, by contiguous spread of renal tumor through the renal capsule, the anterior renal fascia and the posterior parietal peritoneum, or *via* tumoral emboli.

Figure 4 The 62-year-old man with clear cell renal cell carcinoma of the left kidney (stage T1a, grade Ⅱ). A: Transverse plain computed tomography image barely depicts lower pole left kidney mass (arrow), slightly hyperdense. This finding was appreciated after studying the post-contrast enhanced images; B: Coronal reformations during the corticomedullary; C: The nephrographic phase. The tumor (arrow) is seen enhancing strongly and heterogeneously during the corticomedullary phase, a finding strongly suggestive for the diagnosis of renal cell carcinoma (RCC). Hypervascular RCCs as in this case, may enhance to the same degree as the renal cortex and may be mistaken for normal renal parenchyma at the corticomedullary phase. The neoplasm is clearly delineated in the nephrographic phase, detected mainly hypodense, when compared to the contrast-enhancing normal renal parenchyma.

surrounding bones is helpful in guiding the initial surgical incision. Delineation of tumor location and depth of extension into the kidney, ensures maximal preservation of the surrounding normal renal parenchyma after surgery (Figure 6). The arterial and venous anatomy of the kidney is clearly depicted at 3D-CT angiography (Figure 2). Identification of renal vessels, possible anatomic variants and depiction of their relationship with the neoplasm may help minimize ischemic injuries and intraoperative complications. Depiction of the relationship of RCC to the collecting system and assessment of possible neoplastic infiltration represent valuable information in treatment planning, especially in cases of conservative surgery. The pelvicaliceal system is best visualized on coronal MPRs and volume rendering 3D-displays, with images closely resembling those of conventional intravenous urography[47-51].

CT findings of RCC

Most RCCs are solid tumors with CT density of 20 HU or greater at unenhanced scanning[4,28-33]. The tumor may not be clearly visible on plain images, because its density is usually similar to that of the surrounding normal renal parenchyma. In these cases, a focal bulging of the renal contour (Figure 7) may raise the suspicion of a space-occupying lesion. Small tumors (smaller than 3 cm in diameter) are usually homogeneous, while larger lesions tend to be more heterogeneous due to the presence of central necrosis and/or hemorrhage (Figures 3 and 5). Calcifications are seen in up to 30% of RCCs (Figure 5A).

RCC typically has a rich vascular supply[4,28-33]. Therefore, the hallmark diagnosis of RCC is the presence of strong, mainly heterogeneous contrast enhancement (Figures 2-6 and 8). A contrast enhancement value of more than 20 HU with respect to the noncontrast scan is

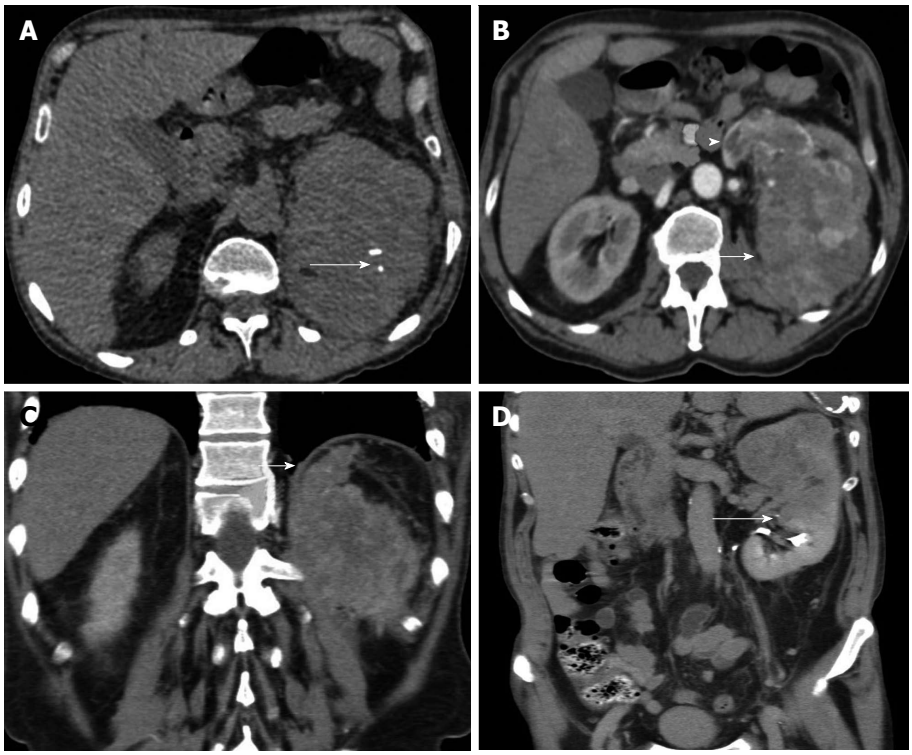

Figure 5 The 62-year-old man with clear cell renal cell carcinoma of the left kidney (stage T3a, grade 3). A: Transverse unenhanced computed tomography (CT) image shows large heterogenous left renal mass, with small areas of calcifications (long arrow); B: Transverse multiplanar reformation (MPR) during the corticomedullary phase demonstrates left renal malignancy (arrow), inhomogeneously enhancing. The left renal vein is dilated and enhances heterogeneously (arrowhead) due to neoplastic invasion. VTT enhances with a same pattern as renal cell carcinoma; C: Coronal reformations during the corticomedullary phase depicts tumor ill-defined margins and extension into the perinephric fat tissue (arrow). Thickening of the diaphragms of the perinephric space is also seen; D: Coronal MPR during the excretory phase shows nonvisualization of the upper calyces and invasion of the middle calyceal group (arrow), a finding strongly suggestive of invasion of renal sinus fat. CT findings were confirmed both surgically and pathologically.

considered suspicious for malignancy. An enhancement value between 10 and 20 HU, is considered indeterminate[45]. On the nephrographic phase, RCCs typically appear hypodense compared to the normally enhancing renal parenchyma (Figure 4).

DIFFERENTIATION OF RCC FROM BENIGN RENAL TUMORS

The wide use of cross-sectional imaging studies has also led to an increase of incidentally discovered benign renal masses, including angiomyolipoma (AML) and renal oncocytoma. Because radical nephrectomy is not desirable for a benign tumor, the accurate characterization of renal masses is required to avoid unwanted surgery. CT findings may prove helpful in characterizing the nature of renal tumors[53-62].

AML can be accurately diagnosed on CT, by detecting the intratumoral fat component with negative density on unenhanced scanning. However, in approximately 4.5% of all AMLs intratumoral fat cannot be visualized at CT. Kim *et al*[53] in a retrospective study of 19 AMLs with minimal fat and 62 RCCs on two-phase helical CT, reported that homogeneous tumor enhancement and prolonged enhancement pattern were the most valuable CT findings in differentiating these tumors, more often detected in the first group. Hyperdensity of a renal mass on plain CT images is another CT finding reported for AML with minimal fat[54]. Zhang *et al*[56] in a retrospective study of 44 AMLs with minimal fat and papillary RCCs reported that the unenhanced CT density, the presence of intratumoural vessels, and the CT density of early excretory phase images may be used to differentiate these tumors. Woo *et al*[57] reported unenhanced tumor-kidney CT density difference and long-to-short axis ratio as the simplest and more accurate features in differentiating AMLs with minimal fat from non-clear cell RCCs on three-phase MDCT.

Several studies have described CT imaging features of renal oncocytoma, including well-defined margins, homogeneous contrast enhancement, presence of a central stellate scar, spoke-wheel pattern of arterial enhancement and absence of hemorrhage, calcifications and necrosis[58,59]. More specifically, renal oncocytoma has been described as a sharply-demarcated solid homogeneous mass, with homogeneous contrast enhancement, except for a hypodense stellate, central area. However, these classic findings do not always allow a confident characterization of this tumor, because they are often seen in patients with RCC[58,59]. MDCT improved the diagnostic performance of CT in differentiating these tumors[60-62]. The enhancement and washout values

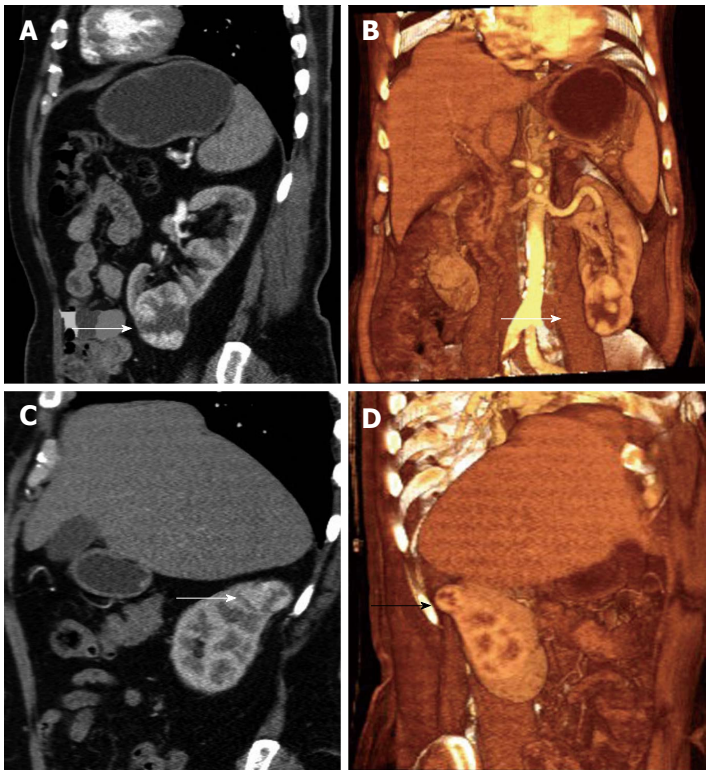

Figure 6 The 74-year-old man with synchronous bilateral renal cell carcinomas of clear cell type (stage T1). Bilateral synchronous renal cell carcinomas (RCCs) are uncommon, reported in less than 2% of patients with RCCs. The patient had left radical nephrectomy and right partial nephrectomy. Sagittal multiplanar reformations (MPR) (A) and coronal 3D reformation with volume rendering technique (B) during the corticomedullary phase depict a sharly-demarcated tumor in the lower pole of the left kidney (arrow, A), strongly and heterogeneously enhancing. Sagittal (C) MPR and (D) 3D reformation with the same algorithm depict a second, smaller tumor in the upper pole of the right kidney, with a similar pattern of contrast enhancement. Preoperative information obtained with computed tomography examination enabled conservative surgery for the right renal malignancy.

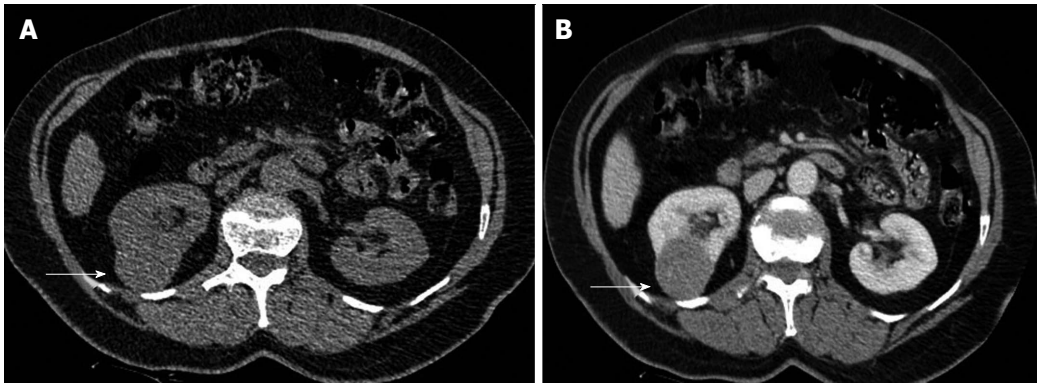

Figure 7 The 60-year-old woman with clear cell renal cell carcinoma of the left kidney (stage T1a, grade Ⅱ). A: Transverse plain computed tomography (CT) image depicts lower pole right renal mass as a focal bulging of the renal contour (arrow), mainly isodense (CT density: 35 HU) to the renal parenchyma; B: Axial multiplanar reformation during the corticomedullary phase clearly shows renal malignancy (arrow) moderately and heterogeneously enhancing (mean CT density: 60 HU). Heterogeneous contrast enhancement on imaging should always suggest renal malignancy preoperatively.

in MDCT may aid in distinguishing small oncocytomas from RCCs of similar size[60,61]. Bird *et al*[60] reported that early phase enhancement greater than 500% and washout values of greater than 50% were mostly seen in renal oncocytomas. Kim *et al*[62] reported characteristic contrast enhancement patterns for renal oncocytomas smaller than 4 cm in diameter on MDCT. The authors assessed segmental enhancement inversion during the corticomedullary phase and early excretory phase, defined as follows: in a renal mass showing two parts with different degrees of enhancement during corticomedullary phase, the relatively more enhanced part became less enhanced during early excretory phase, whereas the less-enhanced part during corticomedullary phase became highly enhanced during early excretory phase. Segmental enhancement inversion was found to be characteristic of small renal oncocytomas in this study[62].

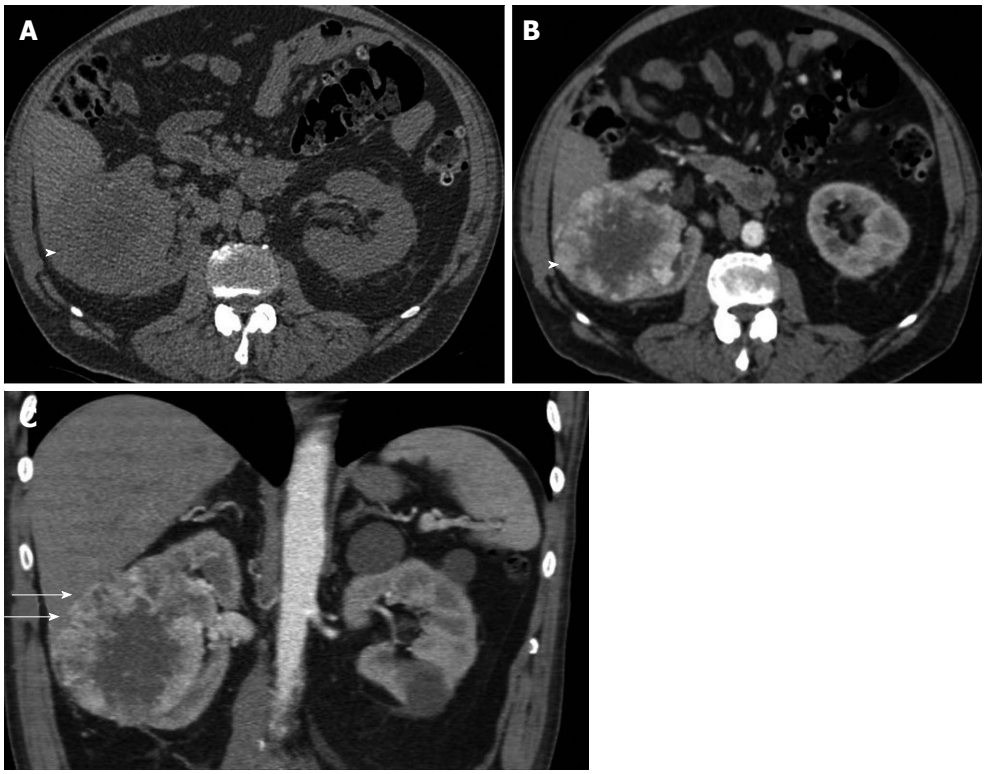

Figure 8 The 75-year-old man with clear cell renal cell carcinoma of the right kidney, invading the liver. A: Axial plain image shows right heterogeneous right renal tumor (arrowhead); B: Transverse reformation during the corticomedullary phase depicts strong, heterogeneous mass enhancement. The tumor (arrowhead) enhances mainly in the periphery, with a mean computed tomography density of 110 HU (compared to that of 40 HU on the unenhanced images), a finding more compatible with the diagnosis of renal cell carcinoma of the clear cell variety. Central non-enhancing areas corresponded to areas of necrosis on pathology; C: Coronal reformation during the same phase shows renal tumor invading the liver (small arrows), a finding confirmed both on surgery and histopathology.

HISTOLOGIC CHARACTERIZATION OF RCC

RCC is considered a clinicopathologically heterogeneous disease and is classified into clear cell (conventional), papillary, chromophobe, collecting duct carcinoma, medullary carcinoma, and unclassified type[15-17]. The commonest histologic subtypes are clear cell, papillary, and chromophobe, accounting for 70%-80%, 14%-17%, and 4%-8% of RCCs, respectively. Each subtype is associated with a different prognosis. Clear cell RCC has the worst prognosis, with a 5-year survival rate of 44%-69%, when compared to the 5-year survival rate of 82%-92% for papillary RCC and the 5-year survival of 78%-87% for chromophobe RCC[15-17]. It has been proposed that a preoperative characterization of the histologic type of RCC may lead to improvements in predicting tumor response to treatment, in providing patient counseling, and in individualizing follow-up regimens[16,17].

CT findings have been reported to correlate closely with the histopathologic characteristics of the more common types of RCC[63-73]. Among CT criteria, degree of enhancement proved to be the most valuable parameter[63-69]. More specifically, ccRCCs are more often detected as highly hypervascular tumors (Figures 2-6 and 8), with areas of cystic degeneration and/or necrosis, whereas papillary (Figure 1) and chromophobe (Figure 9) types are usually more homogeneous and hypovascular[63-73]. Kim *et al*[63] studied the helical CT features of 110 RCCs, including tumor size, degree and patterns of enhancement, presence or absence of calcifications and tumor-spreading patterns. Clear cell RCCs showed stronger enhancement than the other histologic types, with a mean CT density of 106 ± 48 HU in the corticomedullary phase and 62 ± 25 HU in the excretory phase. When using 84 HU as the cutoff value in the corticomedullary phase and 44 HU in the excretory phase, the sensitivity and specificity for differentiating ccRCC from the other subtypes were 74% and 100%, 84% and 91%, respectively[63].

Jung *et al*[67] in a study of 149 small RCCs with MDCT, confirmed the presence of heterogeneous and strong contrast enhancement as more suggestive for the diagnosis of ccRCC, than the papillary and the chromophobe type. Young *et al*[68] recently reported their results on the histologic characterization of 277 RCCs with multiphasic MDCT, using up to four phases (unenhanced, corticomedullary, nephrographic, and excretory phase). Clear cell RCCs showed significantly greater enhancement in the corticomedullary phase (mean CT density: 125.0 HU) than do papillary RCCs (53.6 HU), and chromophobe RCCs (73.8 HU), reporting accuracies of 85% and 84%, respectively in their differentiation[68].

During the last 15 years, advances in the study of

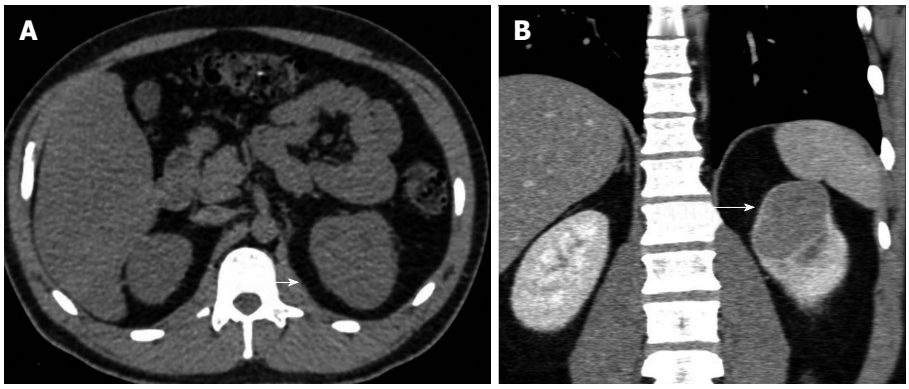

Figure 9 The 31-year-old man with chromophobe renal cell carcinoma of the left kidney (stage T1b, grade Ⅱ). A: Axial plain image barely depicts upper pole left renal mass mainly isodense, with a slight bulging of the renal contour (arrow); B: Coronal reformation during the nephrographic phase clearly depicts left renal tumor (arrow). The neoplasm enhances moderately and homogeneously [computed tomography (CT) density: 70 HU, when compared to the CT density of 35 HU on unenhanced images]. A thin hyperdense rim surrounds renal malignancy, proved to correspond to fibrous pseudocapsule histologically.

ccRCC genetics have led to an improved understanding of the biological characteristics of this tumor, closely correlating with patient's prognosis and to the development of molecular targeted therapies[74-78]. More specifically, the gain of the long arm of chromosome 5 (5q), detected in a sub-set of ccRCCs, correlates with an improved 5-year survival rate and the loss of the short-arm of chromosome 9 (9p) correlates with a lower 5-year survival rate[74-78]. Common chromosomal anomalies in patients with ccRCC also include the loss of the short arm of chromosome 3, the loss of chromosome Y, the gain of the short arm of chromosome 5 and the gain of chromosome 7[73-77]. Sauk *et al*[78] in a retrospective study of 58 histologically proved and karyotyped ccRCCs reported a correlation between multiphasic MDCT features and cytogenetic characteristics of ccRCCs. In their study, ccRCCs with a deletion of chromosome 3p had fewer calcifications than those without this deletion. After contrast material administration, the authors reported greater enhancement for ccRCCs with loss of the Y chromosome than those without the anomaly during the corticomedullary phase (mean CT density: 130.0 HU *vs* 102.5 HU), also for ccRCCs with trisomy 5 than those with disomy 5 during the excretory phase (115.5 HU *vs* 83.4 HU), and for ccRCCs with disomy 7 than those with trisomy 7 during the corticomedullary phase (139.3 HU *vs* 105.8 HU)[78].

GRADING OF RCC

Advances in minimally invasive techniques and active surveillance protocols have allowed treatment of RCC without radical nephrectomy[1]. In these patients, core biopsy can be used to assess the pathologic characteristics of the tumor. However, core biopsy is not always adequate for the assessment of tumor nuclear grade (NG)[79,80]. NG is considered an independent predictor of cancer-specific survival[10-12]. RCCs of high NG are associated with early disease recurrence after therapy and with cancer-related mortality in patients with recurrent disease[10-12]. Therefore, a non-invasive method that could help to predict the histologic characteristics, and more specifically NG in patients with RCC would be valuable. An inverse association between CT tumor enhancement and NG has been reported, with neoplasms of higher NG detected with lower enhancement on multiphasic contrast-enhanced CT examination[81-83]. Villalobos-Gollás *et al*[81] in a retrospective study of 48 RCCs, 44 of which were of clear cell variety evaluated the enhancement of the entire neoplasm on the image with most prominent areas of enhancement. The authors reported an association between higher NG and more advanced-stage disease with areas of lower enhancement of the tumor[81]. Zhu *et al*[80] examined tumor enhancement and relative enhancement values in the corticomedullary and nephrographic phases, by placing a region of interest as large as possible within the solid, more avidly enhancing parts of 255 ccRCCs. Age older than 58 years, irregular tumor margin, and corticomedullary phase relative enhancement value of 0.65 or less were identified as independent predictors of high tumor NG[80]. One possible explanation for the negative association between CT enhancement and NG is the presence of histologic necrosis within the tumor. Histologic necrosis has been reported to correlate with tumor aggressiveness, including higher NG and stage and larger size at diagnosis[80].

RCC SIZE

Tumor size is a significant part of the current TNM staging system[1,9]. It represents a highly important predictor of pathologic stage and survival in RCC[84,85]. Moreover, the selection of appropriate candidates for NSS, along with ablative therapies and active follow-up has been largely guided by tumor sizes evaluated by imaging modalities.

Although, some reports have shown a certain degree of discrepancy between the preoperative CT size of renal tumors and the pathologic size[86,87], discrepancies are minimal and clinically insignificant in most cases[88-90]. Chen *et al*[88] in a study of 169 renal tumors treated with NSS reported an overestimation of renal tumor

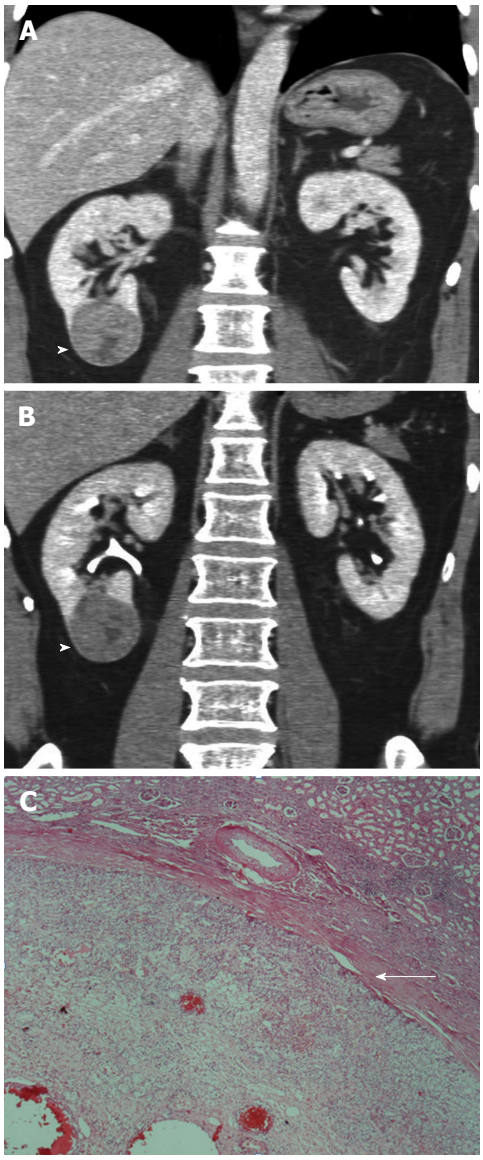

Figure 10 The 50-year-old man with clear cell-chromophobe renal cell carcinoma of right kidney (grade 3, pT1b). A: Coronal reformatted images in corticomedullary; B: Nephrographic phases depict hyperdense rim (arrowhead) surrounding the tumor; C: Histologic section (H and E, × 400) shows fibrous pseudocapsule (arrow) between tumor and adjacent normal renal parenchyma.

size by CT, as compared with the histopathology report. But the discrepancy was only 0.22 cm with little clinical significance, suggesting that CT is an accurate method to measure renal tumor size preoperatively[88]. Choi *et al*[89] in a study of 175 localized RCCs on a 16-row CT scanner, reported a good correlation between the CT and pathologic tumor sizes, although an overestimation of the size was observed for tumors less than 6 cm in diameter. Lee *et al*[90] in a retrospective study of 435 RCCs compared the radiographic tumor size, defined as the largest diameter measured on CT images with the pathologic size. Although, the authors found that CT size overestimated pathologic size, the observed differences were minimal, less than 1 mm, even for small-sized RCCs (4-5 cm in diameter, for which the discrepancies were only about 2 mm), and therefore insignificant[90].

STAGING OF RCC

RCC confined to renal capsule

RCCs generally do not have a true histologic capsule, but are surrounded by a pseudocapsule[91]. The presence of a pseudocapsule surrounding RCC is considered as a histologic feature of early-stage disease[1,91]. These neoplasms are often of small size and of low grade[1,91]. Pseudocapsule formation is the result of tumor growth, producing compression, ischemia, and necrosis of the adjacent renal parenchyma, and resulting in deposition of fibrous tissue[91,92].

MRI has been reported as an accurate technique in the detection of renal pseudocapsule, when compared with CT, angiography and gray-scale sonography, with accuracies ranging from 74%-93%[93-96] Pseudocapsule appears as a hypointense rim between the neoplasm and the normal renal parenchyma on T2-weighted images[93-96]. Yamashita *et al*[94] in a study of 54 RCCs reported an accuracy of 74% in the detection of renal pseudocapsule with MRI and T2-weighted images. At contrast-enhanced CT, the psedocapsule was not visible in any tumors in this study, probably due to the similar contrast enhancement by both the pseudocapsule and the surrounding renal parenchyma[94]. Takahashi *et al*[95] assessed the diagnostic performance of multidetctor CT, selective angiography and MRI in the detection of renal pseudocapsule in 42 RCCs. A pseudocapsule was detected on 26% of neoplasms on CT, as a hypodense or hyperdense rim surrounding RCC, on 67% of neoplasms on angiography, as a radiolucent rim and on 93% of tumors on T2-weighted sequences on MRI, as a low signal intensity rim[95]. Contrast-enhanced sonography improved the diagnostic performance of conventional ultrasound in the preoperative detection of renal pseudocapsule[97]. A sensitivity of 85.7% has been reported by Ascenti *et al*[97] with sonographic contrast agents, detecting pseudocapsule, as a contrast-enhancing rim, surrounding the tumor, usually with late enhancement.

Multiphase MDCT improved the diagnostic performance of CT in the detection of this finding[98]. A retrospective study of 29 RCCs reported an accuracy of 83% in the detection of renal pseudocapsule with MDCT. In this study a four-phase (unenhanced, arterial, portal and nephrographic-excretory phase) CT protocol and multiplanar reformations in the transverse, coronal and sagittal planes of each post-contrast phase were used for CT data interpretation. Portal and nephrographic phase, with coronal and sagittal reformations proved more accurate in the detection of this finding. Renal pseudocapsule was mainly detected as a hyperdense rim surrounding RCC, seen on both phases (Figures 2A, 9B and 10) and this was due to the presence of fibrous tissue. In four cases, a hypodense renal pseudocapsule was revealed (Figure 11) detected only on portal phase

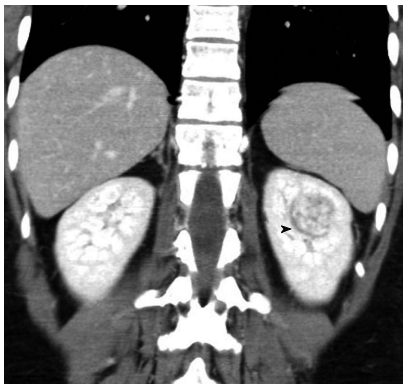

Figure 11 The 44-year-old woman with clear cell renal cell carcinoma of left kidney (grade 2, pT1a). Computed tomography image demonstrates hypodense rim (arrowhead) around neoplasm detected only on coronal reformations during portal phase. The presence of pseudocapsule was confirmed on histology.

reformations[98].

Spread to perinephric tissues

The TNM classification system characterizes advanced RCC within Gerota's fascia as T3. T3a stage RCCs are characterized by tumor grossly invading the renal vein or its segmental branches, or invading perinephric (PN) fat and/or renal sinus (RS) fat[1]. RCCs with PN fat invasion have to penetrate the renal capsule, and tumors with RS fat invasion directly invade the RS fat, due to lack of any capsule at this area. The presence of either PN fat invasion or RS fat invasion, and invasion of both renal fat compartments were significantly associated with synchronous nodal or distant metastases, higher tumor grade and greater tumor dimensions, when compared to patients with no PN fat invasion[99]. Siddiqui *et al*[99] in a retrospective study of 163 pT3a RCCs concluded that PN and RS fat infiltration was associated with death from RCC independent of tumor size. Infiltration of the perinephric fat is also a crucial point when planning NSS. Radical nephrectomy is mandatory in these patients[1].

Perirenal or perinephric space is a cone-shaped retroperitoneal compartment, which is bounded by the anterior (Gerota's fascia) and posterior (Zuckerkandl's facsia) layers of the renal fascia and contains the kidney, adrenal gland, proximal ureter, a prominent amount of fat, a rich network of perirenal vessels and lymphatics, and small-sized lymph nodes[100,101].

The renal fascia measures 1-3 mm in thickness, and the posterior layer is thicker and more often visualized than the anterior layer[100,101]. Thickening of the renal fascia is a sensitive but nonspecific sign, indicating either neoplastic or non-neoplastic adjacent diseases[100,101]. Perinephric space is divided into multiple compartments by thin fibrous lamellae and bridging septa[102]. Kunin[102] described three groups of septa. Group Ⅰ septa arise from the renal capsule and extend to the renal fascia. Group Ⅱ septa are attached to the renal capsule, paralleling more or less the renal surface. Group Ⅲ represents the commonest type, connecting the anterior and posterior leaves of the perinephric space[102]. Thickening of the bridging septa (perinephric stranding) is not a reliable or specific sign in diagnosing neoplastic infiltration of the PN fat tissue[100,101]. A variety of neoplastic and nonneoplastic processes, may involve the perirenal space, including RCC, inflammation, edema, vascular engorgement, hematoma, or fat necrosis[100,101]. Perinephric stranding is also reported in about half of RCCs confined within the kidney.

Detection of PN fat invasion in RCC and differentiation between T1/T2 and T3a stages was the commonest staging error with spiral CT[5,33]. CT criteria used to diagnose neoplastic invasion of PN fat include the following: thickening of the renal fascia, thickening of the bridging septa (perinephric stranding), presence of fluid, presence of peritumoral vessels, defined as asymmetrically enlarged, often irregular vessels within Gerota's fascia, tumor margins and presence of neoplastic nodules within the PN fat, enhancing after contrast material administration[33,103-106]. Multiphase MDCT with multiplanar reformations improved the diagnostic performance of CT in detecting PN fat infiltration[33,103-106]. Catalano *et al*[33] by using three-phase MDCT protocol with thin slices reported an overall accuracy of 95% in diagnosing PN fat invasion, using the presence of hyperdense streaks and nodules surrounding RCC as CT signs to suggest neoplastic infiltration. Kim *et al*[105,106] reported high accuracies for MDCT in detecting PN fat invasion, using tumor size, irregular tumor margins and nodular appearance of the PN fat, as predictors for PN fat invasion. In a retrospective study of 48 RCCs on a 16-row CT scanner, the most significant predictors in diagnosing PN fat invasion were the presence of contrast-enhancing nodules in the PN fat and tumoral margins, with an overall accuracy of 85.4%, for both CT criteria (Figures 3B and 5C)[103].

The renal sinus is a central compartment formed by the extension of the PN space into the medial surface of renal parenchyma. The fibrous capsule terminates at the RS region, resulting in the absence of any barrier preventing the extension of neoplastic cells into the rich network of lymphatics vessels and veins within the RS[107]. RS fat invasion is associated with aggressive tumors at increased risk for dissemination. Thompson *et al*[108] showed that ccRCCs invading the RS fat are more aggressive that tumors with PN fat infiltration only. These neoplasms were more likely to have high NG, regional lymph node metastases and sarcomatoid differentiation. CT criteria used to diagnose invasion of RS fat include the following: extension to the renal sinus, proximity to the pelvicaliceal system, and invasion of the pelvicaliceal system[103]. Among them, renal collecting system invasion was proved to be the single most significant predictor of RS fat invasion (Figure 5D)[103]. None of the other two CT signs proved reliable in the diagnosis of RS fat infiltration. Some RCCs may distort the RS complex and protrude, without signs of invasion. The proximity of a tumor to a neighboring structure, as

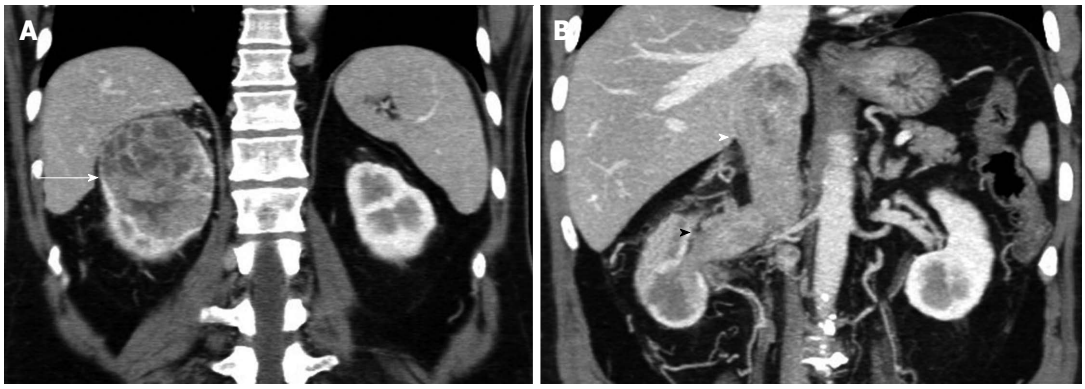

Figure 12 The 64-year-old man with clear cell renal cell carcinoma of the right kidney, invading the renal vein and the inferior vena cava (stage T3b, grade 3). A: Coronal multiplanar reformations during the corticomedullary phase depicts large, inhomegeneously enhancing right renal tumor (arrow); B: Coronal 3D-display with maximum intensity projection technique during the same phase shows neoplastic thrombus invading left renal vein and the inferior vena cava (arrowheads). Coronal reformations clearly show venous invasion extending below the level of the diaphragm. Perinephric stranding and abnormal vessels are detected in the ipsilateral perinephric space, although pathology was negative for perinephric fat invasion.

the pelvicaliceal system, does not always correspond to neoplastic infiltration on histopathology[103].

Venous extension

Extension of RCC into the renal vein alone (stage T3a) occurs in approximately 23% of patients[4]. Tumor involvement of the inferior vena cava (T3b, T3c) is seen in approximately 4%-10% of patients and is more common in right-sided tumors[4]. A venous tumour thrombus (VTT) into the inferior vena cava in patients with RCC is a significant adverse prognostic factor[1]. Excision of the VTT is recommended in patients with non-metastatic RCC[1]. Accurate preoperative evaluation for the presence and extent of the VTT in the renal vein and/or the inferior vena cava is important for planning the appropriate surgical approach for thrombectomy, and minimizing the risk of intraoperative tumoral embolism[4,28-33,109-112]. The level of involvement of the inferior vena cava, whether infrahepatic, retrohepatic or supradiaphragmatic dictates the mode of surgical approach[113].

MDCT has been reported as highly accurate in the diagnosis of spread of RCC into the renal vein, with a reported negative predictive value of 97% and a positive predictive value of 92%[4,28-33,109-112]. MDCT is also effective in delineating the superior extent of inferior vena cava thrombus, with staging results similar to that of MRI[4,28-33,109-112]. Venous extension is optimally detected during the corticomedullary phase, when contrast enhancement of the venous system is maximal. The use of combination of axial images and multiplanar reconstructions is necessary for the assessment of the extension of VTT. The most specific sign of venous invasion is the presence of a low-attenuation filling defect within the vein. The CT characteristics of the thrombus help differentiate neoplastic from bland thrombus. Direct continuity of the thrombus with the primary malignancy suggests metastatic invasion. Heterogeneous enhancement of the thrombus, with a pattern similar to that of RCC also indicates tumoral thrombus (Figures 1B, 1C, 5B and 12)[4,28-33,109-112]. An abrupt change in the caliber of the vein and/or the presence of a clot within collateral veins are considered as ancillary findings suggesting neoplastic involvement. Enlargement of the renal vein alone is not a reliable sign, since it may be due to increased blood flow within a hypervascular RCC or it may represent a normal variant[4,28-33,109-112].

Invasion of the inferior vena cava wall (T3c) is considered an adverse prognostic sign, with a 5-year survival rate of 25% and 69% for patients with tumor invading the inferior vena cava wall and those with free-floating neoplastic thrombus into the inferior vena cava, respectively[45]. Infiltration of the inferior vena cava wall will also complicate surgical resection, because prosthetic reconstruction is usually needed in these patients[45,114]. Focal enhancement of the vena cava wall, or infiltration of adjacent soft tissues, indicates vena cava wall invasion on CT examination[45].

Local organ invasion (beyond the Gerota's fascia, including contiguous extension into the ipsilateral adrenal gland)

Assessment of the adrenal gland is important in patients with RCC for surgical planning. Multivariate analysis in a prospective study comparing the outcomes of radical or partial nephrectomy with, or without, ipsilateral adrenalectomy showed that upper pole tumor location was not predictive of adrenal involvement, but tumour size was predictive[115]. The current trend is to spare the ipsilateral adrenal gland, because ipsilateral adrenalectomy does not provide a survival advantage[1,115]. Adrenalectomy is justified in cases suspicious for metastatic spread, based on radiographic and/or intra-operative findings[1].

MDCT with multiplanar and 3D-reconstructions provide satisfactory results in assessing possible invasion of the adrenal gland[4,8-33,45]. Visualization of a normal adrenal gland at CT has been reported to be associated with a 100% negative predictive value for tumoral invasion, at pathologic analysis. CT signs that strongly suggest

Figure 13 The 70-year-old man with advanced-stage papillary renal cell carcinoma of the left kidney. Coronal multiplanar reformations during the nephrographic phase show large, mainly cystic left renal mass, with solid contrast-enhancing components (arrowheads). Enlarged retroperitoneal LNs, inhomogeneously enhancing (arrow, A) are detected, compatible with metastatic lymphadenopathy. Liver (arrowhead, B) and right adrenal (long arrow, B) metastases are also seen. All metastatic deposits have a similar pattern of enhancement.

invasion of the adrenal gland include the following: adrenal enlargement, displacement, or nonvisualization; adrenalectomy should be performed in these cases[4,28-33,45].

Direct extension of RCC outside Gerota's fascia and into neighboring organs (stage T4) is not always straightforward to diagnose, unless there is a definite focal change in CT density within the affected organ (Figures 3C and 8). Loss of fat tissue planes and irregular margins between RCC and adjacent organs raise the possibility of neoplastic invasion, although this is not always confirmed on histopathology[4,28-33,45]. Multiplanar and 3D-reconstructions help in depicting the relationship of RCC to the adjacent organs in multiple planes and orientations, therefore improving the diagnostic performance of MDCT[4,28-33,45].

Regional lymph node metastases

The presence of regional lymph node (LN) metastases in RCC implies a poor prognosis, with reported 5-year survival rates of 5%-30%[4]. The role of lymph node dissection in RCC remains controversial[4,116]. In patients with localized RCC, without clinical evidence of LN metastases, lymph node dissection is not recommended[1]. In patients with localized disease and clinically enlarged LNs, the survival benefit of LN dissection is unclear. In these cases, LN dissection is suggested mainly for staging purposes or local control[1]. Clinical assessment of LNs status is based on enlargement of LNs on CT and/or MRI and on intraoperative assessment by direct palpation. However, in patients with clinically enlarged LNs, only less than 20% of clinically positive LNs are confirmed to be metastatic at histologic examination[1].

The main CT criterion to diagnose metastatic LN involvement is the size[4,28-33,45]. Retroperitoneal LNs with a short-axis diameter larger than 1 cm are suspicious for neoplastic invasion (Figure 13). A cutoff value of 1 cm as the upper limit for normal LNs has significant limitations. One is the inability to recognize possible micro-metastases, resulting in false-negative findings in approximately 10% of cases. Furthermore, false-positive findings vary between 3%-43%, mostly due to LN enlargement caused by reactive hyperplasia. The enhancement pattern of the node may also help differentiate reactive from malignant adenopathy; metastatic LNs usually present with heterogeneous enhancement. The presence of a hypodense center after contrast material administration, proved to correspond to necrosis on pathology, is considered a highly specific finding, with a positive predictive value of 100% in diagnosing metastatic lymphadenopathy. LNs enhancement with a pattern similar to that of the primary tumor also signifies metastatic disease (Figure 13).

Distant metastases

Metastatic disease occurs in a significant percentage of patients with RCC. At presentation, 25%-30% of RCCs have distant metastases[1]. A median survival of 6-9 mo has been reported for metastases left untreated and a 2-year survival rate of 10%-20% after treatment. The sites of distant metastases from RCC, in order of decreasing frequency are: lungs (50%-60%), bones (30%-40%), liver (30%-40%), and adrenal gland, contralateral kidney, retroperitoneum, and brain (5% each)[117]. Practically any organ may be affected.

Imaging has an important role in assessing the extent of metastatic disease. CT is considered the examination of choice in the detection of intraabdominal metastases (Figures 3, 13 and 14). Like the primary RCC, metastatic lesions are often hypervascular. The optimal phase for their detection is the corticomedullary phase, because they may be obscured on late-phase images.

CONCLUSION

Multidetector multiphase CT with multiplanar and 3D-displays remains the primary imaging modality for the detection of RCC, with high staging accuracies. CT features may prove useful in differentiating RCC from benign renal tumors. CT examination may help in the preoperative characterization of the histologic subtype of RCC. Tumor enhancement patterns of ccRCC

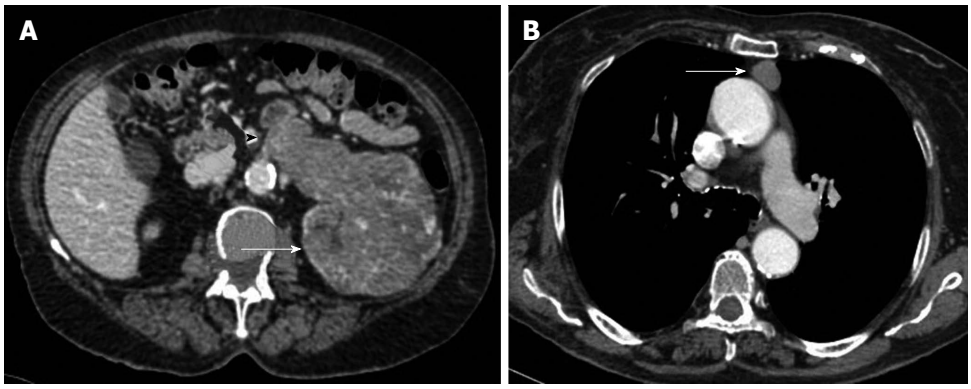

Figure 14 The 81-year-old woman with advanced-stage clear cell renal cell carcinoma of the left kidney. A: Transverse multiplanar reformation during the nephrographic phase shows large, inhomogeneously enhancing left renal malignancy (arrow), invading the ipsilateral renal vein (arrowhead); B: Contrast-enhanced computed tomography image of the thorax demonstrates enlarged mediastinal lymph nodes (arrow), with heterogeneous enhancement, suggestive for metastatic invasion.

are associated with Fuhrman grade and cytogenetic characteristics.

REFERENCES

1 **Ljungberg B**, Bensalah K, Bex A, Canfield S, Dabestani S, Hofmann F, Hora M, Kuczyk MA, Lam T, Volpe A; European Association of Urology. Guidelines on renal cell carcinoma. 2014. Available from: URL: http://uroweb.org/guideline/renal-cell-carcinoma/

2 **Ferlay J**, Steliarova-Foucher E, Lortet-Tieulent J, Rosso S, Coebergh JW, Comber H, Forman D, Bray F. Cancer incidence and mortality patterns in Europe: estimates for 40 countries in 2012. *Eur J Cancer* 2013; **49**: 1374-1403 [PMID: 23485231 DOI: 10.1016/j.ejca.2012.12.027]

3 **American Cancer Society**. Cancer facts and figures 2014. Available from: URL: http://www.cancer.org/acs/groups/content/@research/documents/webcontent/acspc-042151.pdf

4 **Sheth S**, Scatarige JC, Horton KM, Corl FM, Fishman EK. Current concepts in the diagnosis and management of renal cell carcinoma: role of multidetector ct and three-dimensional CT. *Radiographics* 2001; **21** Spec No: S237-S254 [PMID: 11598260 DOI: 10.1148/radiographics.21.suppl_1.g01oc18s237]

5 **Lee CT**, Katz J, Fearn PA, Russo P. Mode of presentation of renal cell carcinoma provides prognostic information. *Urol Oncol* 2002; **7**: 135-140 [PMID: 12474528 DOI: 10.1016/j.purol.2011.02.013]

6 **Patard JJ**, Leray E, Rodriguez A, Rioux-Leclercq N, Guillé F, Lobel B. Correlation between symptom graduation, tumor characteristics and survival in renal cell carcinoma. *Eur Urol* 2003; **44**: 226-232 [PMID: 12875943 DOI: 10.1016/j.eururo.2008.07.053]

7 **Northrup BE**, Jokerst CE, Grubb RL, Menias CO, Khanna G, Siegel CL. Hereditary renal tumor syndromes: imaging findings and management strategies. *AJR Am J Roentgenol* 2012; **199**: 1294-1304 [PMID: 23169721 DOI: 10.2214/AJR.12.9079]

8 **Choyke PL**, Glenn GM, Walther MM, Zbar B, Linehan WM. Hereditary renal cancers. *Radiology* 2003; **226**: 33-46 [PMID: 12511666 DOI: 10.1148/radiol.2261011296]

9 **Eggener S**. TNM staging for renal cell carcinoma: time for a new method. *Eur Urol* 2010; **58**: 517-519; discussion 519-521 [PMID: 20728266 DOI: 10.1016/j.eururo.2010.08.007]

10 **Fuhrman SA**, Lasky LC, Limas C. Prognostic significance of morphologic parameters in renal cell carcinoma. *Am J Surg Pathol* 1982; **6**: 655-663 [PMID: 7180965 DOI: 10.1186/2193-1801-2-378]

11 **Zisman A**, Pantuck AJ, Dorey F, Said JW, Shvarts O, Quintana D, Gitlitz BJ, deKernion JB, Figlin RA, Belldegrun AS. Improved prognostication of renal cell carcinoma using an integrated staging system. *J Clin Oncol* 2001; **19**: 1649-1657 [PMID: 11250993 DOI: 10.1016/j.purol.2009.07.007]

12 **Rioux-Leclercq N**, Karakiewicz PI, Trinh QD, Ficarra V, Cindolo L, de la Taille A, Tostain J, Zigeuner R, Mejean A, Patard JJ. Prognostic ability of simplified nuclear grading of renal cell carcinoma. *Cancer* 2007; **109**: 868-874 [PMID: 17262800]

13 **Sun M**, Lughezzani G, Jeldres C, Isbarn H, Shariat SF, Arjane P, Widmer H, Pharand D, Latour M, Perrotte P, Patard JJ, Karakiewicz PI. A proposal for reclassification of the Fuhrman grading system in patients with clear cell renal cell carcinoma. *Eur Urol* 2009; **56**: 775-781 [PMID: 19573980 DOI: 10.1016/j.eururo.2009.06.008]

14 **Eble JN**, Sauter G, Epstein JI, Sesterhenn IA. Pathology and genetics of tumours of the urinary system and male genital organs. Lyon, France: IARC Press, 2004

15 **Prasad SR**, Humphrey PA, Catena JR, Narra VR, Srigley JR, Cortez AD, Dalrymple NC, Chintapalli KN. Common and uncommon histologic subtypes of renal cell carcinoma: imaging spectrum with pathologic correlation. *Radiographics* 2006; **26**: 1795-1806; discussion 1806-1810 [PMID: 17102051 DOI: 10.1148/rg.266065010]

16 **Cheville JC**, Lohse CM, Zincke H, Weaver AL, Blute ML. Comparisons of outcome and prognostic features among histologic subtypes of renal cell carcinoma. *Am J Surg Pathol* 2003; **27**: 612-624 [PMID: 12717246 DOI: 10.1309/AJCPLBK9L9KDYQZP]

17 **Patard JJ**, Leray E, Rioux-Leclercq N, Cindolo L, Ficarra V, Zisman A, De La Taille A, Tostain J, Artibani W, Abbou CC, Lobel B, Guillé F, Chopin DK, Mulders PF, Wood CG, Swanson DA, Figlin RA, Belldegrun AS, Pantuck AJ. Prognostic value of histologic subtypes in renal cell carcinoma: a multicenter experience. *J Clin Oncol* 2005; **23**: 2763-2771 [PMID: 15837991 DOI: 10.1200/JCO.2005.07.055]

18 **Novick AC**. Renal-sparing surgery for renal cell carcinoma. *Urol Clin North Am* 1993; **20**: 277-282 [PMID: 8493750 DOI: 10.1016/j.juro.2011.02]

19 **Van Poppel H**, Bamelis B, Oyen R, Baert L. Partial nephrectomy for renal cell carcinoma can achieve long-term tumor control. *J Urol* 1998; **160**: 674-678 [PMID: 9720519 DOI: 10.1016/S0022-5347(01)62751-4]

20 **Krejci KG**, Blute ML, Cheville JC, Sebo TJ, Lohse CM, Zincke H. Nephron-sparing surgery for renal cell carcinoma: clinicopathologic features predictive of patient outcome. *Urology* 2003; **62**: 641-646 [PMID: 14550434 DOI: 10.1016/S0090-4295(03)00489-8]

21 **Zincke H**, Ghavamian R. Partial nephrectomy for renal cell cancer is here to stay--more data on this issue. *J Urol* 1998; **159**: 1161-1162 [PMID: 9507822 DOI: 10.1097/00005392-199804000-00013]

22 **MacLennan S**, Imamura M, Lapitan MC, Omar MI, Lam TB, Hilvano-Cabungcal AM, Royle P, Stewart F, MacLennan G, MacLennan SJ, Canfield SE, McClinton S, Griffiths TR, Ljungberg B, N'Dow J. Systematic review of oncological outcomes following

surgical management of localised renal cancer. *Eur Urol* 2012; **61**: 972-993 [PMID: 22405593 DOI: 10.1016/j.eururo.2012.02.039]
23 **Gratzke C**, Seitz M, Bayrle F, Schlenker B, Bastian PJ, Haseke N, Bader M, Tilki D, Roosen A, Karl A, Reich O, Khoder WY, Wyler S, Stief CG, Staehler M, Bachmann A. Quality of life and perioperative outcomes after retroperitoneoscopic radical nephrectomy (RN), open RN and nephron-sparing surgery in patients with renal cell carcinoma. *BJU Int* 2009; **104**: 470-475 [PMID: 19239445 DOI: 10.1111/j.1464-410X.2009.08439.x]
24 **Van Poppel H**, Da Pozzo L, Albrecht W, Matveev V, Bono A, Borkowski A, Colombel M, Klotz L, Skinner E, Keane T, Marreaud S, Collette S, Sylvester R. A prospective, randomised EORTC intergroup phase 3 study comparing the oncologic outcome of elective nephron-sparing surgery and radical nephrectomy for low-stage renal cell carcinoma. *Eur Urol* 2011; **59**: 543-552 [PMID: 21186077 DOI: 10.1016/j.eururo.2010.12.013]
25 **Whitson JM**, Harris CR, Meng MV. Population-based comparative effectiveness of nephron-sparing surgery vs ablation for small renal masses. *BJU Int* 2012; **110**: 1438-1443; discussion 1443 [PMID: 22639860 DOI: 10.1111/j.1464-410X.2012.11113.x]
26 **Jewett MA**, Mattar K, Basiuk J, Morash CG, Pautler SE, Siemens DR, Tanguay S, Rendon RA, Gleave ME, Drachenberg DE, Chow R, Chung H, Chin JL, Fleshner NE, Evans AJ, Gallie BL, Haider MA, Kachura JR, Kurban G, Fernandes K, Finelli A. Active surveillance of small renal masses: progression patterns of early stage kidney cancer. *Eur Urol* 2011; **60**: 39-44 [PMID: 21477920 DOI: 10.1016/j.eururo.2011.03.030]
27 **Abouassaly R**, Lane BR, Novick AC. Active surveillance of renal masses in elderly patients. *J Urol* 2008; **180**: 505-508; discussion 508-509 [PMID: 18550113 DOI: 10.1016/j.juro.2008.04.033]
28 **Pavlica P**, Derchi L, Martorana G, Bertaccini A, Pavlica P, Martorana G, Barozzi L. Renal Cell Carcinoma Imaging. *Eur Urol Sup* 2006; **5**: 580-592 [DOI: 10.1016/j.eursup.2006.03.010]
29 **Heidenreich A**, Ravery V. Preoperative imaging in renal cell cancer. *World J Urol* 2004; **22**: 307-315 [PMID: 15290202 DOI: 10.1590/S1677-55382007000300002]
30 **Coll DM**, Smith RC. Update on radiological imaging of renal cell carcinoma. *BJU Int* 2007; **99**: 1217-1222 [PMID: 17441914 DOI: 10.1111/j.1464-410X.2007.06824.x]
31 **Gardner TA**, Tirkes T, Mellon M, Koch MO. Imaging techniques for the patient with renal cell carcinoma. *Semin Nephrol* 2011; **31**: 245-253 [PMID: 21784273 DOI: 10.1016/j.semnephrol.2011.05.004]
32 **Kang SK**, Kim D, Chandarana H. Contemporary imaging of the renal mass. *Curr Urol Rep* 2011; **12**: 11-17 [PMID: 20949339 DOI: 10.1007/s11934-010-0148-y]
33 **Catalano C**, Fraioli F, Laghi A, Napoli A, Pediconi F, Danti M, Nardis P, Passariello R. High-resolution multidetector CT in the preoperative evaluation of patients with renal cell carcinoma. *AJR Am J Roentgenol* 2003; **180**: 1271-1277 [PMID: 12704036 DOI: 10.2214/ajr.180.5]
34 **Johnson PT**, Horton KM, Fishman EK. How not to miss or mischaracterize a renal cell carcinoma: protocols, pearls, and pitfalls. *AJR Am J Roentgenol* 2010; **194**: W307-W315 [PMID: 20308475 DOI: 10.2214/AJR.09.3033]
35 **Silverman SG**, Lee BY, Seltzer SE, Bloom DA, Corless CL, Adams DF. Small (< or = 3 cm) renal masses: correlation of spiral CT features and pathologic findings. *AJR Am J Roentgenol* 1994; **163**: 597-605 [PMID: 8079852 DOI: 10.2214/ajr.163.3.8079852]
36 **Zhang J**, Lefkowitz RA, Ishill NM, Wang L, Moskowitz CS, Russo P, Eisenberg H, Hricak H. Solid renal cortical tumors: differentiation with CT. *Radiology* 2007; **244**: 494-504 [PMID: 17641370]
37 **Hsu RM**, Chan DY, Siegelman SS. Small renal cell carcinomas: correlation of size with tumor stage, nuclear grade, and histologic subtype. *AJR Am J Roentgenol* 2004; **182**: 551-557 [PMID: 14975944 DOI: 10.2214/ajr.182.3.1820551]
38 **Kopka L**, Fischer U, Zoeller G, Schmidt C, Ringert RH, Grabbe E. Dual-phase helical CT of the kidney: value of the corticomedullary and nephrographic phase for evaluation of renal lesions and preoperative staging of renal cell carcinoma. *AJR Am J Roentgenol* 1997; **169**: 1573-1578 [PMID: 9393168]
39 **Birnbaum BA**, Jacobs JE, Ramchandani P. Multiphasic renal CT: comparison of renal mass enhancement during the corticomedullary and nephrographic phases. *Radiology* 1996; **200**: 753-758 [PMID: 8756927 DOI: 10.1148/radiology.200.3.8756927]
40 **Yuh BI**, Cohan RH. Different phases of renal enhancement: role in detecting and characterizing renal masses during helical CT. *AJR Am J Roentgenol* 1999; **173**: 747-755 [PMID: 10470916 DOI: 10.2214/ajr.173.3.10470916]
41 **Cohan RH**, Sherman LS, Korobkin M, Bass JC, Francis IR. Renal masses: assessment of corticomedullary-phase and nephrographic-phase CT scans. *Radiology* 1995; **196**: 445-451 [PMID: 7617859 DOI: 10.1148/radiology.196.2.7617859]
42 **Johnson CD**, Dunnick NR, Cohan RH, Illescas FF. Renal adenocarcinoma: CT staging of 100 tumors. *AJR Am J Roentgenol* 1987; **148**: 59-63 [PMID: 3491524 DOI: 10.2214/ajr.148.1.59]
43 **Hallscheidt PJ**, Bock M, Riedasch G, Zuna I, Schoenberg SO, Autschbach F, Soder M, Noeldge G. Diagnostic accuracy of staging renal cell carcinomas using multidetector-row computed tomography and magnetic resonance imaging: a prospective study with histopathologic correlation. *J Comput Assist Tomogr* 2004; **28**: 333-339 [PMID: 15100536 DOI: 10.1097/00004728-200405000-00005]
44 **Hallscheidt P**, Wagener N, Gholipour F, Aghabozorgi N, Dreyhaupt J, Hohenfellner M, Haferkamp A, Pfitzenmaier J. Multislice computed tomography in planning nephron-sparing surgery in a prospective study with 76 patients: comparison of radiological and histopathological findings in the infiltration of renal structures. *J Comput Assist Tomogr* 2006; **30**: 869-874 [PMID: 17082687 DOI: 10.1097/01.rct.0000230009.31715.5b]
45 **Türkvatan A**, Akdur PO, Altinel M, Olçer T, Turhan N, Cumhur T, Akinci S, Ozkul F. Preoperative staging of renal cell carcinoma with multidetector CT. *Diagn Interv Radiol* 2009; **15**: 22-30 [PMID: 19263370]
46 **Ganeshan D**, Morani A, Ladha H, Bathala T, Kang H, Gupta S, Lalwani N, Kundra V. Staging, surveillance, and evaluation of response to therapy in renal cell carcinoma: role of MDCT. *Abdom Imaging* 2014; **39**: 66-85 [PMID: 24077815 DOI: 10.1007/s00261-013-0040-6]
47 **Zagoria RJ**, Bechtold RE, Dyer RB. Staging of renal adenocarcinoma: role of various imaging procedures. *AJR Am J Roentgenol* 1995; **164**: 363-370 [PMID: 7839970 DOI: 10.2214/ajr.164.2.7839970]
48 **Coll DM**, Herts BR, Davros WJ, Uzzo RG, Novick AC. Preoperative use of 3D volume rendering to demonstrate renal tumors and renal anatomy. *Radiographics* 2000; **20**: 431-438 [PMID: 10715341 DOI: 10.1148/radiographics.20.2.g00mc16431]
49 **Coll DM**, Uzzo RG, Herts BR, Davros WJ, Wirth SL, Novick AC. 3-dimensional volume rendered computerized tomography for preoperative evaluation and intraoperative treatment of patients undergoing nephron sparing surgery. *J Urol* 1999; **161**: 1097-1102 [PMID: 10081846 DOI: 10.4103/0974-7796.134256]
50 **Ueda T**, Tobe T, Yamamoto S, Motoori K, Murakami Y, Igarashi T, Ito H. Selective intra-arterial 3-dimensional computed tomography angiography for preoperative evaluation of nephron-sparing surgery. *J Comput Assist Tomogr* 2004; **28**: 496-504 [PMID: 15232381 DOI: 10.1097/00004728-200407000-00010]
51 **Smith PA**, Marshall FF, Corl FM, Fishman EK. Planning nephron-sparing renal surgery using 3D helical CT angiography. *J Comput Assist Tomogr* 1999; **23**: 649-654 [PMID: 10524840]
52 **American College of Radiology**. ACR Appropriateness Criteria: Urologic Imaging. Renal cell carcinoma staging. [Accessed 2011 January 26]. Available from: URL: http://www.acr.org/
53 **Kim JK**, Park SY, Shon JH, Cho KS. Angiomyolipoma with minimal fat: differentiation from renal cell carcinoma at biphasic helical CT. *Radiology* 2004; **230**: 677-684 [PMID: 14990834 DOI: 10.1148/radiol.2303030003]
54 **Jinzaki M**, Tanimoto A, Narimatsu Y, Ohkuma K, Kurata T, Shinmoto H, Hiramatsu K, Mukai M, Murai M. Angiomyolipoma: imaging findings in lesions with minimal fat. *Radiology* 1997; **205**:

497-502 [PMID: 9356635 DOI: 10.1148/radiology.205.2.9356635]
55 **Obuz F**, Karabay N, Seçil M, Igci E, Kovanlikaya A, Yörükoglu K. Various radiological appearances of angiomyolipomas in the same kidney. *Eur Radiol* 2000; **10**: 897-899 [PMID: 10879697 DOI: 10.1007/s003300051031]
56 **Zhang YY**, Luo S, Liu Y, Xu RT. Angiomyolipoma with minimal fat: differentiation from papillary renal cell carcinoma by helical CT. *Clin Radiol* 2013; **68**: 365-370 [PMID: 23321146 DOI: 10.1016/j.crad.2012.08.028]
57 **Woo S**, Cho JY, Kim SH, Kim SY. Angiomyolipoma with minimal fat and non-clear cell renal cell carcinoma: differentiation on MDCT using classification and regression tree analysis-based algorithm. *Acta Radiol* 2014; **55**: 1258-1269 [PMID: 24259298 DOI: 10.1177/0284185113513887]
58 **Jasinski RW**, Amendola MA, Glazer GM, Bree RL, Gikas PW. Computed tomography of renal oncocytomas. *Comput Radiol* 1985; **9**: 307-314 [PMID: 4064635 DOI: 10.1016/0730-4862(85)90057-5]
59 **Davidson AJ**, Hayes WS, Hartman DS, McCarthy WF, Davis CJ. Renal oncocytoma and carcinoma: failure of differentiation with CT. *Radiology* 1993; **186**: 693-696 [PMID: 8430176 DOI: 10.1148/radiology.186.3.8430176]
60 **Bird VG**, Kanagarajah P, Morillo G, Caruso DJ, Ayyathurai R, Leveillee R, Jorda M. Differentiation of oncocytoma and renal cell carcinoma in small renal masses (< 4 cm): the role of 4-phase computerized tomography. *World J Urol* 2011; **29**: 787-792 [PMID: 20717829 DOI: 10.1007/s00345-010-0586-7]
61 **Gakis G**, Kramer U, Schilling D, Kruck S, Stenzl A, Schlemmer HP. Small renal oncocytomas: differentiation with multiphase CT. *Eur J Radiol* 2011; **80**: 274-278 [PMID: 20667676 DOI: 10.1016/j.ejrad.2010.06.049]
62 **Kim JI**, Cho JY, Moon KC, Lee HJ, Kim SH. Segmental enhancement inversion at biphasic multidetector CT: characteristic finding of small renal oncocytoma. *Radiology* 2009; **252**: 441-448 [PMID: 19508984 DOI: 10.2214/AJR.12.8616]
63 **Kim JK**, Kim TK, Ahn HJ, Kim CS, Kim KR, Cho KS. Differentiation of subtypes of renal cell carcinoma on helical CT scans. *AJR Am J Roentgenol* 2002; **178**: 1499-1506 [PMID: 12034628 DOI: 10.2214/ajr.178.6.1781499]
64 **Herts BR**, Coll DM, Novick AC, Obuchowski N, Linnell G, Wirth SL, Baker ME. Enhancement characteristics of papillary renal neoplasms revealed on triphasic helical CT of the kidneys. *AJR Am J Roentgenol* 2002; **178**: 367-372 [PMID: 11804895 DOI: 10.2214/ajr.178.2.1780367]
65 **Sheir KZ**, El-Azab M, Mosbah A, El-Baz M, Shaaban AA. Differentiation of renal cell carcinoma subtypes by multislice computerized tomography. *J Urol* 2005; **174**: 451-455; discussion 455 [PMID: 16006863]
66 **Jinzaki M**, Tanimoto A, Mukai M, Ikeda E, Kobayashi S, Yuasa Y, Narimatsu Y, Murai M. Double-phase helical CT of small renal parenchymal neoplasms: correlation with pathologic findings and tumor angiogenesis. *J Comput Assist Tomogr* 2000; **24**: 835-842 [PMID: 11105696 DOI: 10.4103/0973-1482.137924]
67 **Jung SC**, Cho JY, Kim SH. Subtype differentiation of small renal cell carcinomas on three-phase MDCT: usefulness of the measurement of degree and heterogeneity of enhancement. *Acta Radiol* 2012; **53**: 112-118 [PMID: 22114020 DOI: 10.1258/ar.2011.110221]
68 **Young JR**, Margolis D, Sauk S, Pantuck AJ, Sayre J, Raman SS. Clear cell renal cell carcinoma: discrimination from other renal cell carcinoma subtypes and oncocytoma at multiphasic multidetector CT. *Radiology* 2013; **267**: 444-453 [PMID: 23382290]
69 **Bata P**, Gyebnar J, Tarnoki DL, Tarnoki AD, Kekesi D, Szendroi A, Fejer B, Szasz AM, Nyirady P, Karlinger K, Berczi V. Clear cell renal cell carcinoma and papillary renal cell carcinoma: differentiation of distinct histological types with multiphase CT. *Diagn Interv Radiol* 2013; **19**: 387-392 [PMID: 23864331 DOI: 10.5152/dir.2013.13068]
70 **Zokalj I**, Marotti M, Kolarić B. Pretreatment differentiation of renal cell carcinoma subtypes by CT: the influence of different tumor enhancement measurement approaches. *Int Urol Nephrol* 2014; **46**: 1089-1100 [PMID: 24381132 DOI: 10.1007/s11255-013-0631-8]
71 **Lee-Felker SA**, Felker ER, Tan N, Margolis DJ, Young JR, Sayre J, Raman SS. Qualitative and quantitative MDCT features for differentiating clear cell renal cell carcinoma from other solid renal cortical masses. *AJR Am J Roentgenol* 2014; **203**: W516-W524 [PMID: 25341166 DOI: 10.2214/AJR.14.12460]
72 **Pierorazio PM**, Hyams ES, Tsai S, Feng Z, Trock BJ, Mullins JK, Johnson PT, Fishman EK, Allaf ME. Multiphasic enhancement patterns of small renal masses (≤4 cm) on preoperative computed tomography: utility for distinguishing subtypes of renal cell carcinoma, angiomyolipoma, and oncocytoma. *Urology* 2013; **81**: 1265-1271 [PMID: 23601445 DOI: 10.1016/j.urology.2012.12.049]
73 **Veloso Gomes F**, Matos AP, Palas J, Mascarenhas V, Herédia V, Duarte S, Ramalho M. Renal cell carcinoma subtype differentiation using single-phase corticomedullary contrast-enhanced CT. *Clin Imaging* 2014; **39**: 273-277 [PMID: 25457534 DOI: 10.1016/j.clinimag.2014]
74 **Gunawan B**, Huber W, Holtrup M, von Heydebreck A, Efferth T, Poustka A, Ringert RH, Jakse G, Füzesi L. Prognostic impacts of cytogenetic findings in clear cell renal cell carcinoma: gain of 5q31-qter predicts a distinct clinical phenotype with favorable prognosis. *Cancer Res* 2001; **61**: 7731-7738 [PMID: 11691785]
75 **Presti JC**, Wilhelm M, Reuter V, Russo P, Motzer R, Waldman F. Allelic loss on chromosomes 8 and 9 correlates with clinical outcome in locally advanced clear cell carcinoma of the kidney. *J Urol* 2002; **167**: 1464-1468 [PMID: 11832771 DOI: 10.1002/cncr.25279]
76 **Mitsumori K**, Kittleson JM, Itoh N, Delahunt B, Heathcott RW, Stewart JH, McCredie MR, Reeve AE. Chromosome 14q LOH in localized clear cell renal cell carcinoma. *J Pathol* 2002; **198**: 110-114 [PMID: 12210070 DOI: 10.1002/path.1165]
77 **Brunelli M**, Eccher A, Gobbo S, Ficarra V, Novara G, Cossu-Rocca P, Bonetti F, Menestrina F, Cheng L, Eble JN, Martignoni G. Loss of chromosome 9p is an independent prognostic factor in patients with clear cell renal cell carcinoma. *Mod Pathol* 2008; **21**: 1-6 [PMID: 17906617 DOI: 10.1038/modpathol.3800967]
78 **Sauk SC**, Hsu MS, Margolis DJ, Lu DS, Rao NP, Belldegrun AS, Pantuck AJ, Raman SS. Clear cell renal cell carcinoma: multiphasic multidetector CT imaging features help predict genetic karyotypes. *Radiology* 2011; **261**: 854-862 [PMID: 22025734 DOI: 10.1148/radiol.11101508]
79 **Lane BR**, Samplaski MK, Herts BR, Zhou M, Novick AC, Campbell SC. Renal mass biopsy--a renaissance? *J Urol* 2008; **179**: 20-27 [PMID: 17997455 DOI: 10.1016/j.juro.2009.01.061]
80 **Zhu YH**, Wang X, Zhang J, Chen YH, Kong W, Huang YR. Low enhancement on multiphase contrast-enhanced CT images: an independent predictor of the presence of high tumor grade of clear cell renal cell carcinoma. *AJR Am J Roentgenol* 2014; **203**: W295-W300 [PMID: 25148187]
81 **Villalobos-Gollás M**, Aguilar-Davidov B, Culebro-García C, Gómez-Alvarado MO, Rojas-Garcia P, Ibarra-Fombona R, Uribe-Uribe N, Feria-Bernal G, Castillejos-Molina R, Sotomayor M, Gabilondo F, Rodríguez-Covarrubias F. Pathological implications of areas of lower enhancement on contrast-enhanced computed tomography in renal-cell carcinoma: additional information for selecting candidates for surveillance protocols. *Int Urol Nephrol* 2012; **44**: 1369-1374 [PMID: 22648292 DOI: 10.1007/s11255-012-0199-8]
82 **Wang JH**, Min PQ, Wang PJ, Cheng WX, Zhang XH, Wang Y, Zhao XH, Mao XQ. Dynamic CT Evaluation of Tumor Vascularity in Renal Cell Carcinoma. *AJR Am J Roentgenol* 2006; **186**: 1423-1430 [PMID: 16632740 DOI: 10.2214/AJR.04.1408]
83 **Birnbaum BA**, Bosniak MA, Krinsky GA, Cheng D, Waisman J, Ambrosino MM. Renal cell carcinoma: correlation of CT findings with nuclear morphologic grading in 100 tumors. *Abdom Imaging* 1994; **19**: 262-266 [PMID: 8019359 DOI: 10.1007/BF00203523]
84 **Karakiewicz PI**, Lewinshtein DJ, Chun FK, Briganti A, Guille F, Perrotte P, Lobel B, Ficarra V, Artibani W, Cindolo L, Tostain J, Abbou CC, Chopin D, De La Taille A, Patard JJ. Tumor size

improves the accuracy of TNM predictions in patients with renal cancer. *Eur Urol* 2006; **50**: 521-528; discussion 529 [PMID: 16530322 DOI: 10.1016/j.eururo.2006.02.034]

85 **Steiner T**, Knels R, Schubert J. Prognostic significance of tumour size in patients after tumour nephrectomy for localised renal cell carcinoma. *Eur Urol* 2004; **46**: 327-330 [PMID: 15306102 DOI: 10.1016/j.eururo.2004.06]

86 **Schlomer B**, Figenshau RS, Yan Y, Bhayani SB. How does the radiographic size of a renal mass compare with the pathologic size? *Urology* 2006; **68**: 292-295 [PMID: 16904439]

87 **Kurta JM**, Thompson RH, Kundu S, Kaag M, Manion MT, Herr HW, Russo P. Contemporary imaging of patients with a renal mass: does size on computed tomography equal pathological size? *BJU Int* 2009; **103**: 24-27 [PMID: 18710440 DOI: 10.1111/j.1464-410X.2008.07941.x]

88 **Chen W**, Wang L, Yang Q, Liu B, Sun Y. Comparison of radiographic and pathologic sizes of renal tumors. *Int Braz J Urol* 2013; **39**: 189-194 [PMID: 23683665 DOI: 10.1590/S1677-5538.IBJU.2013.02.06]

89 **Choi JY**, Kim BS, Kim TH, Yoo ES, Kwon TG. Correlation between Radiologic and Pathologic Tumor Size in Localized Renal Cell Carcinoma. *Korean J Urol* 2010; **51**: 161-164 [PMID: 20414390 DOI: 10.4111/kju.2010.51.3.161]

90 **Lee SE**, Lee WK, Kim DS, Doo SH, Park HZ, Yoon CY, Hwang SI, Lee HJ, Choe G, Hong SK. Comparison of radiographic and pathologic sizes of renal tumors. *World J Urol* 2010; **28**: 263-267 [PMID: 20119641]

91 **Minervini A**, di Cristofano C, Lapini A, Marchi M, Lanzi F, Giubilei G, Tosi N, Tuccio A, Mancini M, della Rocca C, Serni S, Bevilacqua G, Carini M. Histopathologic analysis of peritumoral pseudocapsule and surgical margin status after tumor enucleation for renal cell carcinoma. *Eur Urol* 2009; **55**: 1410-1418 [PMID: 18692300 DOI: 10.1016/j.eururo.2008.07.038]

92 **Huang SQ**, Zou SS, Huang QL. MR appearance of the pseudocapsule of renal cell carcinoma and its pathologic basis. *Urol Radiol* 1992; **13**: 158-161 [PMID: 1539405 DOI: 10.1007/BF02924611]

93 **Yamashita Y**, Takahashi M, Watanabe O, Yoshimatsu S, Ueno S, Ishimaru S, Kan M, Takano S, Ninomiya N. Small renal cell carcinoma: pathologic and radiologic correlation. *Radiology* 1992; **184**: 493-498 [PMID: 1620854 DOI: 10.1148/radiology.184.2.1620854]

94 **Yamashita Y**, Honda S, Nishiharu T, Urata J, Takahashi M. Detection of pseudocapsule of renal cell carcinoma with MR imaging and CT. *AJR Am J Roentgenol* 1996; **166**: 1151-1155 [PMID: 8615260 DOI: 10.2214/AJR.08.1727]

95 **Takahashi S**, Ueda J, Furukawa T, Higashino K, Tsujihata M, Itatani H, Narumi Y, Nakamura H. Renal cell carcinoma: preoperative assessment for enucleative surgery with angiography, CT, and MRI. *J Comput Assist Tomogr* 1996; **20**: 863-870 [PMID: 8933783 DOI: 10.1007/s11604-009-0347-y]

96 **Roy C**, El Ghali S, Buy X, Lindner V, Lang H, Saussine C, Jacqmin D. Significance of the pseudocapsule on MRI of renal neoplasms and its potential application for local staging: a retrospective study. *AJR Am J Roentgenol* 2005; **184**: 113-120 [PMID: 15615960 DOI: 10.2214/ajr.184.1.01840113]

97 **Ascenti G**, Gaeta M, Magno C, Mazziotti S, Blandino A, Melloni D, Zimbaro G. Contrast-enhanced second-harmonic sonography in the detection of pseudocapsule in renal cell carcinoma. *AJR Am J Roentgenol* 2004; **182**: 1525-1530 [PMID: 15150001 DOI: 10.2214/ajr.182.6.1821525]

98 **Tsili AC**, Argyropoulou MI, Gousia A, Kalef-Ezra J, Sofikitis N, Malamou-Mitsi V, Tsampoulas K. Renal cell carcinoma: value of multiphase MDCT with multiplanar reformations in the detection of pseudocapsule. *AJR Am J Roentgenol* 2012; **199**: 379-386 [PMID: 22826400 DOI: 10.2214/AJR.11.7747]

99 **Siddiqui SA**, Frank I, Leibovich BC, Cheville JC, Lohse CM, Zincke H, Blute ML. Impact of tumor size on the predictive ability of the pT3a primary tumor classification for renal cell carcinoma. *J Urol* 2007; **177**: 59-62 [PMID: 17162000 DOI: 10.1016/j.juro.2006.08.069]

100 **Bechtold RE**, Dyer RB, Zagoria RJ, Chen MY. The perirenal space: relationship of pathologic processes to normal retroperitoneal anatomy. *Radiographics* 1996; **16**: 841-854 [PMID: 8835975 DOI: 10.1148/radiographics.16.4.8835975]

101 **Surabhi VR**, Menias C, Prasad SR, Patel AH, Nagar A, Dalrymple NC. Neoplastic and non-neoplastic proliferative disorders of the perirenal space: cross-sectional imaging findings. *Radiographics* 2008; **28**: 1005-1017 [PMID: 18635626 DOI: 10.1148/rg.284075157]

102 **Kunin M**. Bridging septa of the perinephric space: anatomic, pathologic, and diagnostic considerations. *Radiology* 1986; **158**: 361-365 [PMID: 3941862 DOI: 10.1148/radiology.158.2.3941862]

103 **Tsili AC**, Goussia AC, Baltogiannis D, Astrakas L, Sofikitis N, Malamou-Mitsi V, Argyropoulou MI. Perirenal fat invasion on renal cell carcinoma: evaluation with multidetector computed tomography-multivariate analysis. *J Comput Assist Tomogr* 2013; **37**: 450-457 [PMID: 23674020 DOI: 10.1097/RCT.0b013e318283bc8e]

104 **Hedgire SS**, Elmi A, Nadkarni ND, Cao K, McDermott S, Harisinghani MG. Preoperative evaluation of perinephric fat invasion in patients with renal cell carcinoma: correlation with pathological findings. *Clin Imaging* 2013; **37**: 91-96 [PMID: 23206613 DOI: 10.1016/j.clinimag.2012.03.005]

105 **Kim C**, Choi HJ, Cho KS. Diagnostic performance of multidetector computed tomography in the evaluation of perinephric fat invasion in renal cell carcinoma patients. *J Comput Assist Tomogr* 2014; **38**: 268-273 [PMID: 24448501 DOI: 10.1097/RCT.0b013e3182aa672a]

106 **Kim C**, Choi HJ, Cho KS. Diagnostic value of multidetector computed tomography for renal sinus fat invasion in renal cell carcinoma patients. *Eur J Radiol* 2014; **83**: 914-918 [PMID: 24713489 DOI: 10.1016/j.ejrad.2014.02.025]

107 **Rha SE**, Byun JY, Jung SE, Oh SN, Choi YJ, Lee A, Lee JM. The renal sinus: pathologic spectrum and multimodality imaging approach. *Radiographics* 2004; **24** Suppl 1: S117-S131 [PMID: 15486236 DOI: 10.1148/rg.24si045503]

108 **Thompson RH**, Leibovich BC, Cheville JC, Webster WS, Lohse CM, Kwon ED, Frank I, Zincke H, Blute ML. Is renal sinus fat invasion the same as perinephric fat invasion for pT3a renal cell carcinoma? *J Urol* 2005; **174**: 1218-1221 [PMID: 16145373 DOI: 10.1097/01.ju.0000173942.19990.40]

109 **Hallscheidt PJ**, Fink C, Haferkamp A, Bock M, Luburic A, Zuna I, Noeldge G, Kauffmann G. Preoperative staging of renal cell carcinoma with inferior vena cava thrombus using multidetector CT and MRI: prospective study with histopathological correlation. *J Comput Assist Tomogr* 2005; **29**: 64-68 [PMID: 15665685 DOI: 10.1097/01.rct.0000146113.56194.6d]

110 **Sokhi HK**, Mok WY, Patel U. Stage T3a renal cell carcinoma: staging accuracy of CT for sinus fat, perinephric fat or renal vein invasion. *Br J Radiol* 2015; **88**: 20140504 [PMID: 25410425 DOI: 10.1259/bjr.20140504]

111 **Guzzo TJ**, Pierorazio PM, Schaeffer EM, Fishman EK, Allaf ME. The accuracy of multidetector computerized tomography for evaluating tumor thrombus in patients with renal cell carcinoma. *J Urol* 2009; **181**: 486-490; discussion 491 [PMID: 19100567]

112 **Stern Padovan R**, Perkov D, Smiljanic R, Oberman B, Potocki K. Venous spread of renal cell carcinoma: MDCT. *Abdom Imaging* 2005; **32**: 530-537 [PMID: 16947069 DOI: 10.1007/s00261-006-9088-x]

113 **Staehler G**, Brkovic D. The role of radical surgery for renal cell carcinoma with extension into the vena cava. *J Urol* 2000; **163**: 1671-1675 [PMID: 10799157 DOI: 10.1590/S1677-55382009000600003]

114 **Schimmer C**, Hillig F, Riedmiller H, Elert O. Surgical treatment of renal cell carcinoma with intravascular extension. *Interact Cardiovasc Thorac Surg* 2004; **3**: 395-397 [PMID: 17670271 DOI: 10.1016/j.icvts.2004.02.014]

115 **Lane BR**, Tiong HY, Campbell SC, Fergany AF, Weight CJ, Larson BT, Novick AC, Flechner SM. Management of the adrenal gland during partial nephrectomy. *J Urol* 2009; **181**: 2430-2436; discussion 2436-2437 [PMID: 19371896 DOI: 10.1016/j.juro.2009.02.027]

116 **Bekema HJ**, MacLennan S, Imamura M, Lam TB, Stewart F,

Scott N, MacLennan G, McClinton S, Griffiths TR, Skolarikos A, MacLennan SJ, Sylvester R, Ljungberg B, N'Dow J. Systematic review of adrenalectomy and lymph node dissection in locally advanced renal cell carcinoma. *Eur Urol* 2013; **64**: 799-810 [PMID: 23643550 DOI: 10.1016/j.eururo.2013.04.033]

117 **Griffin N**, Gore ME, Sohaib SA. Imaging in metastatic renal cell carcinoma. *AJR Am J Roentgenol* 2007; **189**: 360-370 [PMID: 17646462 DOI: 10.2214/AJR.07.2077]

P- Reviewer: Liu HM, Vinh-Hung V, Yuan Z **S- Editor**: Tian YL
L- Editor: A **E- Editor**: Liu SQ

Published by **Baishideng Publishing Group Inc**
8226 Regency Drive, Pleasanton, CA 94588, USA
Telephone: +1-925-223-8242
Fax: +1-925-223-8243
E-mail: bpgoffice@wjgnet.com
Help Desk: http://www.wjgnet.com/esps/helpdesk.aspx
http://www.wjgnet.com